

Journal of Biomedical Optics

BiomedicalOptics.SPIEDigitalLibrary.org

Medical laser application: translation into the clinics

Ronald Sroka
Herbert Stepp
Georg Hennig
Gary M. Brittenham
Adrian Rühm
Lothar Lilge

Medical laser application: translation into the clinics

Ronald Sroka,^{a,*} Herbert Stepp,^a Georg Hennig,^a Gary M. Brittenham,^b Adrian Rühm,^a and Lothar Lilge^c

^aLaser-Forschungslabor, LIFE Center, University Hospital of Munich, Feodor-Lynen-Str 19, D-81377 Munich, Germany

^bColumbia University, College of Physicians and Surgeons, Children's Hospital of New York, Room CHN 10-08, 3959 Broadway, New York, New York 10032, United States

^cUniversity of Toronto, Princess Margaret Cancer Centre, Medical Biophysics, 101 College Street 15-310, Toronto, Ontario M5G 1L7, Canada

Abstract. Medical laser applications based on widespread research and development is a very dynamic and increasingly popular field from an ecological as well as an economic point of view. Conferences and personal communication are necessary to identify specific requests and potential unmet needs in this multi- and interdisciplinary discipline. Precise gathering of all information on innovative, new, or renewed techniques is necessary to design medical devices for introduction into clinical applications and finally to become established for routine treatment or diagnosis. Five examples of successfully addressed clinical requests are described to show the long-term endurance in developing light-based innovative clinical concepts and devices. Starting from laboratory medicine, a noninvasive approach to detect signals related to iron deficiency is shown. Based upon photosensitization, fluorescence-guided resection had been discovered, opening the door for photodynamic approaches for the treatment of brain cancer. Thermal laser application in the nasal cavity obtained clinical acceptance by the introduction of new laser wavelengths in clinical consciousness. Varicose veins can be treated by innovative endoluminal treatment methods, thus reducing side effects and saving time. Techniques and developments are presented with potential for diagnosis and treatment to improve the clinical situation for the benefit of the patient. © 2015 Society of Photo-Optical Instrumentation Engineers (SPIE) [DOI: [10.1117/1.JBO.20.6.061110](https://doi.org/10.1117/1.JBO.20.6.061110)]

Keywords: therapy; diagnostics; optical coherence tomography; photodynamic therapy; otorhinolaryngology; neurosurgery; phlebotomy; laboratory medicine; iron deficiency; varicosis; breast cancer; brain cancer; hypertrophic turbinate.

Paper 140734SSRR received Nov. 6, 2014; accepted for publication May 11, 2015; published online Jun. 16, 2015.

1 Introduction

Medical laser application is a broad area armed with advanced technologies to meet challenges in clinical diagnostics and therapy and to address health care issues that impact broad populations. Recent research and emerging developments provide the vision of improving clinical therapeutic procedures or extending the use of lasers to new fields of medicine. Novel biomedical laser applications and new types of lasers widen the possible spectrum of laser-tissue interactions to improve target-oriented, precise application of laser radiation in clinical practice.

New laser light application techniques as well as innovative medical keyhole techniques are under development or at the translational stage in clinics. Highly sophisticated targeting strategies, including endogenous or applied fluorophores, conjugates of nanoparticles, and antibodies, pave the way for new treatment modalities. Combination therapies such as the synergistic use of photodynamic therapy (PDT) and immune-modulatory agents or antiseptics are new fields for research and clinical studies. Improved understanding of biological reactions triggered by laser radiation interacting with natural absorbing sites, targeting molecules, photosensitizers, or nanoparticles will lead to progress in the creation of minimally invasive clinical laser light applications, or assist in elucidating particular immunological responses of the tissue. Theoretical considerations and modeling of laser light distribution in tissue with subsequent energy transfer and tissue interactions constitute a solid

basis for therapy planning in patients, particularly if combined with improved light delivery and monitoring techniques.

“Medical Laser Applications and Laser-Tissue Interactions” is a subconference during the European Conference on Biomedical Optics held biannually in Munich. Presentations from around the world covering all fields of laser applications in medicine are regularly presented. This conference provides an interdisciplinary forum for scientists, engineers, technicians, and medical doctors using laser-assisted treatment modalities to discuss progress in all these topics. This forum supports presentations ranging from *in vitro* investigations to clinical studies of new laser light irradiation modalities in the range of 10^{-3} to 10^{18} W cm⁻², which can eventually lead to the development of new laser-assisted techniques that can play an important role in the future.

Laser light applications in medicine are based on effects ranging from thermal to nonthermal laser-tissue interactions, which includes ionization effects either on the macro-scale (e.g., in the case of soft tissue smoothing without ablation), on the micro-scale (e.g., in the case of selective retina therapy), or on the nano-scale (e.g., in the case of surgery within cells), as well as short-pulsed laser applications. Generally, both soft and hard tissues can be treated.

There are a variety of medical societies, e.g., ophthalmology, dermatology, and urology, where laser-assisted applications are already part of routine diagnostics and therapy. Here, advancing laser medical applications are summarized, which are close to entering into clinical practice, e.g., noninvasive detection of

*Address all correspondence to: Ronald Sroka, E-mail: Ronald.Sroka@med.uni-muenchen.de

iron deficiency, improvements in the treatment of glioblastoma multiforme (GBM), photonic technologies for breast cancer (BC) management ranging from risk assessment to therapy, minimally invasive endonasal surgery, and endoluminal laser treatment of varicose veins. It is intended to describe the way how unsolved or insufficiently solved problems in clinical medicine can be overcome step-by-step by suitable technical solutions, which requires identifying the white spots as well as bridging the gap between the research bench and bedside.

2 Detection of Iron Deficiency

In the following, we will report about previously published studies.^{1,2} Iron deficiency is a worldwide form of malnutrition, which increases the risk of disability and death. In particular, infants, young children, adolescents, menstruating, and pregnant women often suffer from iron deficiency, which causes anemia and other adverse effects, including impaired cognitive development, decreased immune responsiveness, and, when severe, increased mortality.³ Iron supplementation and food iron fortification are methods to prevent or correct nutritional iron deficiency.³ In the absence of malaria, universal iron supplementation did not affect mortality,⁴ but in a malarial area, it increased the risk of severe illness and death in iron-replete children.^{3,5,6} For this reason, the World Health Organization concluded that universal iron supplementation should not be implemented without screening for iron deficiency.⁶

2.1 Diagnostic Problem

Iron deficiency can be detected by several methods,⁷⁻¹¹ which are invasive and require tissue or blood samples for laboratory analysis. Zinc protoporphyrin-IX (ZnPP), a metallo-porphyrin, is produced during heme biosynthesis when the supply of iron is limited and, therefore, is alternatively formed instead of heme by

ferrochelatase (EC 4.99.1.1) from zinc ions and protoporphyrin-IX (PPIX), yet in a very low concentration, as shown in Fig. 1. Both, ZnPP and PPIX are located within erythrocytes.¹² For diagnostic purposes, the ZnPP/heme ratio is preferred over the absolute concentration of ZnPP (Ref. 12) as the ratio is independent of patient hematocrit. An elevated ZnPP/heme ratio most commonly indicates iron deficiency or lead exposure,¹¹⁻¹⁴ and a lowered ZnPP/heme ratio may be found in hereditary hemochromatosis.^{12,15} The upper threshold for the ZnPP/heme ratio differs between studies and methods but is usually in the range of 40 to 80 $\mu\text{mol ZnPP/mol heme}$.^{7,12,16} Especially in hospitalized patients, the specificity of the ZnPP/heme ratio for nutritional iron deficiency may be influenced by coexisting disorders, such as lead poisoning, anemia of chronic disease, or chronic inflammation.^{7,17,18} In some circumstances, the ZnPP/heme ratio may serve as an index of chronic inflammation and can be used to monitor the effectiveness of treatment.¹⁷

Routinely, ZnPP and PPIX concentrations can be measured by extraction and high-performance liquid chromatography (HPLC) separation^{13,19} and detection by its fluorescence light emission upon blue light excitation. To calculate the ZnPP/heme ratio, additionally a routine Hb measurement is required. A low-cost and rapid method for determining the ZnPP/heme ratio is the use of a portable front-face fluorometer, the hematofluorometer,²⁰ requiring only a drop of (capillary or venous) blood, which directly measures the fluorescence light emitted by the erythrocyte ZnPP. In reasonable approximation, the signal is independent of the hematocrit²⁰ and is a direct measure for the ZnPP/heme ratio.^{20,21} Due to its simplicity, the hematofluorometer is recommended as a screening device for targeted iron supplementation.²² However, the signal detected is influenced by background fluorescence of other blood constituents.^{16,23-27} Potential elimination of background fluorescence entails further requirements, e.g., extended sample preparation time, additional

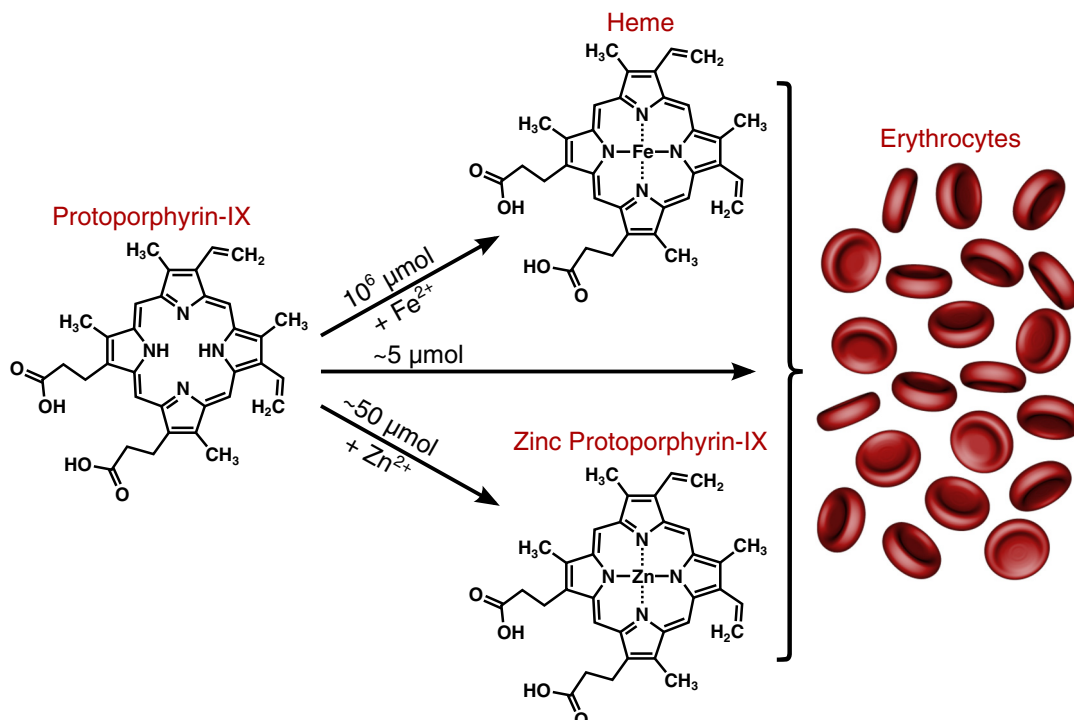


Fig. 1 Synthesis of zinc protoporphyrin-IX (ZnPP) instead of heme in case of Fe deficiency.¹²

laboratory equipment, and trained personnel. The application of this device is thus restricted if cost-effective measurements are needed, laboratory infrastructure is not available, or venipuncture is not feasible, e.g., in the case of point-of-care screening for iron deficiency under field conditions.²²

2.2 Noninvasive Method

A method to measure the ZnPP/heme ratio independent of the background fluorescence is the dual-wavelength excitation method. This technique eliminates the autofluorescence background while retaining the porphyrin fluorescence emission.^{1,2,28} Employing two laser diodes at 407 and 425 nm, it shows potential for field diagnosis while removing the need to wash the erythrocytes prior to ZnPP/heme ratio determination. In Fig. 2, the background-free ZnPP fluorescence signal measured from diluted whole blood is correlated with a reference HPLC measurement.

In further investigations, the dual-wavelength excitation method¹ will be applied to noninvasive autofluorescence measurements to measure the faint erythrocyte ZnPP fluorescence noninvasively. The oral mucosa has been identified as a potential site to conduct these measurements, because the blood vessels are covered only by a thin, nonpigmented epithelial layer, such that light penetration of excitation light is not hindered. The capillary blood density is high, so that a sufficient amount of ZnPP fluorophores can be expected in the illuminated tissue volume. Still, background fluorescence is expected to be an even greater problem than for the whole-blood measurements. Among the main tissue fluorophores are collagen and elastin crosslinks,²⁹ whose fluorescence intensities are assumed to considerably exceed the ZnPP fluorescence signal remitted from tissue surfaces. Therefore, a method to efficiently reduce tissue background fluorescence also would be needed for successful noninvasive ZnPP/heme ratio quantitation. It was shown that the dual-wavelength excitation method eliminated, on average, 92% of the autofluorescence background for 20 subjects.²

In conclusion, these studies showed that the dual-wavelength excitation method successfully eliminates the autofluorescence background in whole blood while retaining the porphyrin fluorescence emission. Therefore, this approach allows for the construction of a simple, inexpensive point-of-care instrument

quantifying the ZnPP/heme ratio from unwashed whole blood. For a future point-of-care instrument that quantifies the ZnPP/heme ratio noninvasively from the oral mucosa, dual-wavelength excitation can be used to largely eliminate the overwhelming tissue autofluorescence background to permit the quantitation of the faint ZnPP fluorescence signal.

3 Treatment of Glioblastoma Multiforme in Neurosurgery

GBM ranks among the oncological diseases with the worst prognosis. At an incidence rate of 3 to 4 per 100,000 people,³⁰ the median survival after initial diagnosis is age-dependent and ranges from 6 to 9 months for older patients to 18 to 21 months for younger patients.³¹ GBM is a devastating disease, despite improvements in survival rates achieved so far, and there is an urgent need for innovative treatment concepts. Survival after surgery and radiotherapy of malignant gliomas is linked to the completeness of tumor removal.³²⁻³⁴ Therefore, methods that permit intraoperative identification of residual tumor tissue may be beneficial. The aim of initial open surgery is to remove most of the tumor volume as indicated by preoperative magnetic resonance imaging (MRI) with contrast agent. There is increasing evidence that “safe gross total resection” is correlated with improved recurrence free survival.³⁵

3.1 Fluorescence-Guided Resection

Several malignant tissues synthesize increased amounts of endogenous porphyrins after exposure to 5-aminolevulinic acid (5-ALA). It has been shown that C6 glioma cells, as a model for human malignant glioma, similarly synthesize porphyrins when exposed to 5-ALA and that selective synthesis occurs when C6 cells are inoculated into rat brains to form a tumor.³⁶ The kinetics of porphyrin fluorescence intensities in cultured C6 cells was investigated by flow cytometry. According to these *in vitro* and *in vivo* experiments, after exposure to 5-ALA, cultured C6 cells show a linear increase of PPIX fluorescence, which begins to plateau after 85 min. Marked fluorescence is also observed in solid and infiltrating experimental tumor. However, faint fluorescence also occurs in normal tissue. Based on these encouraging investigations, first, clinical applications could be envisioned, and subsequently, the benefit of fluorescent porphyrins that accumulate in malignant tissue after administration of a precursor (5-ALA) for labeling of malignant gliomas in patients could be confirmed.³⁷ For doing this intraoperatively, available clinical techniques and equipment from urological fluorescence diagnosis were adapted and transferred.^{38,39} Hence, red porphyrin fluorescence was observed with a 455 nm long-pass filter upon excitation with violet-blue (375 to 440 nm) xenon light, and also quantitatively assessed by analysis of fluorescence spectra.⁴⁰ Fluorescing and nonfluorescing samples taken from the tumor perimeters were examined histologically. Normal brain tissue revealed no porphyrin fluorescence, whereas tumor tissue was distinguished by bright red fluorescence. For a total of 89 tissue biopsies, the sensitivity was 85% and the specificity was 100% for the detection of malignant tissue. For seven of nine patients, visible porphyrin fluorescence led to further resection of the tumor. Photobleaching caused a decay of the fluorescence intensity to 36% in 25 min during violet-blue light excitation and in 87 min during white light exposure. These observations suggested that 5-ALA induced porphyrin fluorescence may label malignant gliomas safely and accurately enough to enhance

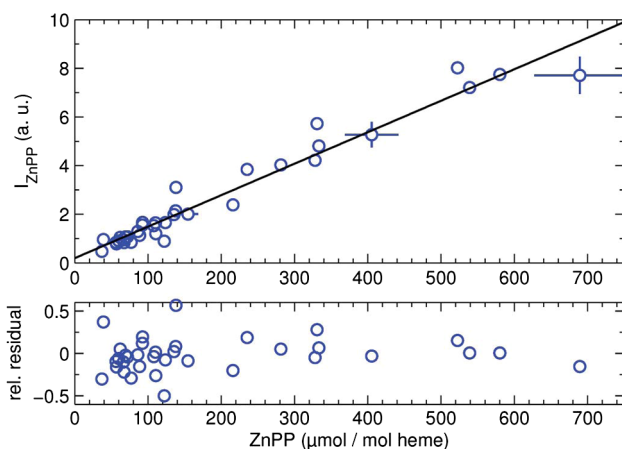


Fig. 2 Correlation of background-free ZnPP fluorescence (y axis) to standard evaluation using high-performance liquid chromatography (x axis).¹

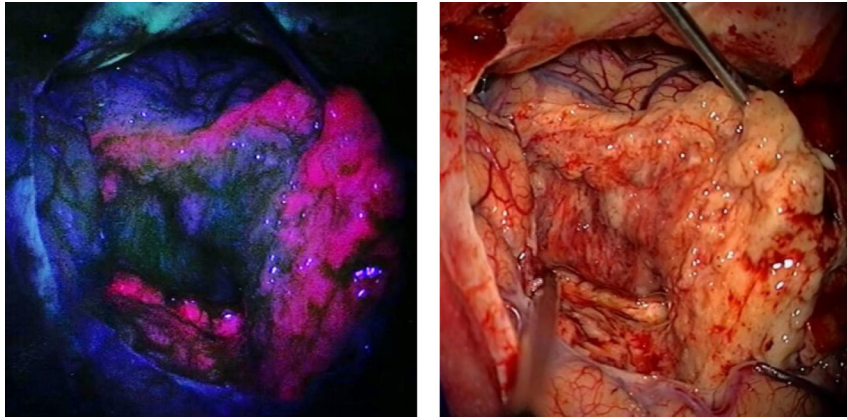


Fig. 3 (a) Red fluorescence of 5-aminolevulinic acid induced protoporphyrin-IX during fluorescence-guided glioblastoma multiforme resection serves for contrast enhancement and allows demarcation of residual tumor tissue with millimeter resolution, thus offering surgeons a precise guidance during resection.⁴⁸ (b) Intraoperative white light view of the same situation.

the completeness of tumor removal. Concurrent developments of neurosurgery-specific optical devices, aimed at improving such fluorescence-guided microsurgical resections of malignant gliomas using surgical microscopes, finally enabled uncomplicated and rapid recognition of the red tumor fluorescence and its borders to normal tissue, without interrupting the course of the surgery. Such systems appeared to constitute a useful tool for optimizing removal of malignant gliomas on a routine basis.^{41,42} Hence, prospective clinical trials involving the fluorescence-guided resection (FGR) technique based on 5-ALA induced PPIX fluorescence were started.^{37,43,44} This technique has meanwhile been evaluated in multicenter clinical trials, and it is nowadays established in a variety of neurosurgery hospitals.⁴³ So far, 5-ALA based FGR in neurosurgery is approved in Australia, Hong Kong, Israel, Taiwan, South Korea, and Japan.

However, even when employing FGR based on 5-ALA induced PPIX, which had proven to exhibit excellent sensitivity and specificity and to considerably facilitate “gross total tumor resections”^{45–48} as shown in Fig. 3, one cannot expect the surgery to be curative, due to the infiltrative nature of the tumor growth.³⁷

3.2 Photodynamic Therapy

Apart from the specific induction of tissue fluorescence, fluorophores such as PPIX may also cause the tissue to be photosensitized. PDT relies on the accumulation of significant amounts of such photosensitizing agents in the diseased tissue, which in combination with properly designed light exposure leads to phototoxic effects in the treated tissue. PDT is increasingly being used amongst health practitioners in combating a variety of diseases.⁴⁹ In the field of 5-ALA based PDT, a variety of clinical approaches are either under investigation or in clinical trials, which include the areas of dermatology, urology, brain, otorhinolaryngology, gynecology, and gastroenterology. In the following, the translation of basic scientific investigations to clinical application is sketched for the case of neurosurgery.

In vitro and *in vivo* investigations showed the potential of 5-ALA induced PPIX as photosensitizer for PDT in C6 glioma cells.^{50–52} This suggests that the PPIX content in tumor tissue observed during FGR could also be exploited for PDT treatment

of glioblastoma, both by surface irradiation of the surgical cavity and/or by stereotactically guided interstitial irradiation. These treatment modalities could be particularly helpful when clinical tumor removal by FGR had to be finished prematurely even though not all red or faintly fluorescing areas had been resected, e.g., because the affected tissue regions were part of eloquent areas. Intraoperative fluorescence spectroscopy showed higher sensitizer concentration in vital brain tumor versus the infiltration zone and in the infiltration zone versus adjacent normal brain, which contained very little PPIX.⁵³ Obviously tumor cells in the infiltration zone can be reached by PDT, which would otherwise be left behind untreated.

While PPIX based PDT is well-established for the treatment of actinic keratosis and basal cell carcinoma,⁵⁴ there are only occasional clinical reports about its application for GBM treatment.⁵⁵ Even in these cases, the photosensitizer Photofrin® has mostly been used in addition, obviously because the surgeons were not trusting in a sufficient phototoxic potential of the accumulated PPIX from 5-ALA alone. A variety of different photosensitizers have meanwhile been investigated for intracranial PDT^{56, 57}; including metronomic PDT.^{58,59} Published clinical experience with PDT for GBM treatment relying solely on 5-ALA induced PPIX is limited.^{60–64} In these trials and individual treatment attempts, PDT was applied by interstitial placement of radial diffusers while relying on the same or only slightly increased 5-ALA dosage as usually used for FGR.

Successful PDT requires homogeneous irradiation and light detection for dosimetry purposes. Irradiation devices for focal PDT of the brain cavity after FGR of the tumor tissue had been developed,⁶⁵ and the accumulation of PPIX in the brain tumor and adjacent tissue had been investigated to improve the PDT effect⁶¹ before interstitial PDT (iPDT) could be applied clinically for the first time.⁶⁶

Limited knowledge about the light, temperature, and photosensitizer distribution within the target volume initially hampered the clinical application of iPDT of gliomas. Monte Carlo (MC) simulations of fluence rate and heat transport resulted in an improved three-dimensional (3-D) treatment planning, which allowed to assess and define the treatment volume more accurately and to optimize the position of the light diffusers within the lesion.⁶⁰ Optical needle endoscopy was

implemented for safe and precise stereotactically guided biopsy sampling in neurosurgery, which may also provide an innovative means to further optimize and individualize the iPDT treatment in the future.⁶⁷

Overall, stereotactic iPDT in combination with treatment planning could be shown to be a safe and feasible treatment modality.⁶⁶ These single-case treatments were extended to also include on-line monitoring of PPIX fluorescence and photobleaching kinetics, which seems important as dramatically different PPIX concentration levels and photobleaching kinetics have been observed. Such data were assessed and analyzed in order to employ them for real-time treatment monitoring and as early prognostic markers for the PDT response of individual patients. With regards to the PPIX concentration, it could be shown that necrotic regions typically located in the center of a GBM tumor are characterized by significantly lower PPIX levels than the outer regions consisting of vital tumor tissue. As indicated by this example, the implementation of fluorescence spectroscopy during iPDT could become a promising tool for individualized treatment concepts.^{61,68,69} The evaluation of such spectroscopic data obtained from interfiber measurements of fluorescence and transmission during clinical stereotactic iPDT showed that the intratumoral PPIX concentration in glioblastoma exhibits pronounced inter- and intratumoral variations, which are directly linked to likewise variable levels of fluorescence intensity.⁶⁴ A high intratumoral PPIX concentration, associated with strong fluorescence intensity and complete photobleaching in the course of an iPDT treatment, also seems to be associated with a favorable treatment outcome. A typical intraoperative situation during an iPDT treatment with real-time monitoring of PPIX fluorescence intensity and photobleaching is shown in Fig. 4. The monitoring procedure turned out to be feasible and might be suitable for early treatment prognosis of iPDT. Furthermore, an individualization of treatment strategy and treatment parameters based on this information appears to bear a potential to further improve the clinical outcomes.^{64,70} Improving all these techniques and the interaction between



Fig. 4 Clinical stereotactic interstitial photodynamic therapy using several fibers ending in cylindrical diffusers for therapeutic light application (e.g., 635 nm). The system is capable of interfiber detection of fluorescence (e.g., 705 nm) and transmission (e.g., 635 nm) for on-line monitoring during treatment.^{64,70}

highly motivated partners may improve the clinical situation for treating GBM in neurosurgery for the benefit of the patients to prolong symptom-free survival with the highest degree of quality of life.⁶⁵

4 Diagnostics/Treatment of Breast Cancer

4.1 Challenge in the Clinical Management of Breast Cancer

BC remains the most common oncological disease for women in North America⁷¹ and worldwide.^{72,73} The challenges BC presents for health care systems and the affected individuals are different in high-income countries where BC screening and therapy are well-established compared to low- and middle-income countries where, particularly for the latter, mammographic screening remains a bottleneck leaving women often nondiagnosed.

In high-income countries, the combination of high participation in mammography screening programs⁷² in combination with advanced therapeutic options have led to a high five-year survival of >90%, for BC patients.⁷¹ In particular, the advanced treatment options comprising surgery, chemotherapy (prior to surgery and postsurgery), and radiation therapy resulted in statistically equal five-year survival times for a nonscreened and a mammographic screened population. This opens the doors to different interpretation concerning the need for mammographic screening. While lowering screening compliance will result in more late-stage tumors, it will also reduce overdiagnosis, thus reducing stress and unnecessary secondary testing, including invasive biopsies in false-positive women. Conversely, the treatment of late-stage BC will increase costs ~20 to 30 times⁷⁴ more than that of stage I/II BC. Additionally, survival statistics beyond five years are not available with adequate repeats to generate final recommendations about BC screening's efficacy. Conversely, while 40- to 50-year-old women have an overall low incidence of BC,⁷² their incidence rates are increasing at the highest rate particularly in countries undergoing a lifestyle change, which is well-documented in South Korea⁷⁵ and also seen in countries such as Mexico and Egypt, although with less-solid data. It is in particular this age group that benefits of the most from early detection of BC as they would face potentially the most life years lost. Hence, improving the selection of women entering a BC screening program and adjusting the screening frequency based on a personalized risk assessment will lead to a better utilization of available screening resources in low- and middle-income countries and hence enable detection of predominantly early-stage BC, thus simultaneously reducing the overall cost burden to these health care systems.

Photonics-based tools for BC detection are still required particularly for premenopausal women and women with high mammographic tissue density as dense glandular and connective tissue hinders the detection of small lesions in the breast. While high-risk BrCa I/II gene mutation carrier are typically imaged every six months, alternatingly with MRI or ultrasound (US), other high-risk women, particularly those with a strong family history of BC or on long-term immune suppression therapy for an unrelated disease, are not given the same considerations. Nonionizing low-cost imaging-based screening is highly desirable for this population. The requirements for these imaging modalities are providing high contrast between glandular and, in particular, malignant tissue, being mostly independent of

connective and fatty tissue. Low cost is desirable for implementation of this technology as standard BC screening technology, particularly in higher-mid- to lower-high-income countries with pending implementation of a national BC screening program, is an urgent task as these countries also currently have the largest gains in life expectancy and, hence, overall increase in BC incidence. Here again if the situation from Korea and Japan repeats itself, the increase will be disproportional in women <50 years of age who are commonly not captured by x-ray based BC

screening. It is noteworthy that this is an economically limited environment, although it encompasses up to 1/4 of the female world population. The needs of these women pertaining to BC screening and early detection are unlikely to be met with current x-ray based technology including tomosynthesis as this is aimed primarily on the highest-income countries; see Table 1 (modified from Ref. 76).

A field where an adoption of photonics-based imaging tools is anticipated and highly likely is for neoadjuvant chemotherapy

Table 1 Breast cancer screening programs in 26 ICSN countries in 2012.

| Region/country | Year program began | Detection methods in routine use | Age groups covered | Recommended interval for average risk for mammography | Number of women screened (2010) | Participation rate (2010) age 40 to 49 |
|----------------------------|--------------------|----------------------------------|--------------------|---|---------------------------------|--|
| Australia | 1991 | MM, DM | 40 to 75+ | 2 years | Data not available | Data not available |
| Canada | 1988 | MM, DM, CBE | 50 to 69 | 1 year | 196,187 | 47.30% |
| China | 2009 | MM, CBE, U | 40 to 59 | 3 years | 1,200,000 | Data not available |
| Denmark | 1991 | DM | 50 to 69 | NA | 275,000 | 73.00% |
| Finland | 1987 | DM | 50 to 64 | NA | Data not available | 85.00% |
| France | 1989 | MM, DM, CBE | 50 to 74 | NA | 2,343,980 | 52.30% |
| Iceland | 1987 | DM, CBE | 40 to 69 | 2 years | Data not available | 60.00% |
| Israel | 1997 | MM, DM | 50 to 74 | NA | 220,000 | 72.00% |
| Italy | 2002 | MM, DM | 50 to 69 | NA | 1,340,311 | 60.50% |
| Japan | 1977 | MM, DM, CBE | 40 to 75+ | 2 years | 2,492,868 | 19.00% |
| Korea | 1999 | MM, DM | 40 to 75+ | 2 years | 2,602,928 | 39.30% |
| Luxembourg | 1992 | DM | 50 to 69 | NA | 14,586 | 64.00% |
| Netherlands | 1989 | MM, DM | 50 to 74 | NA | 961,766 | 80.70% |
| New Zealand | 1998 | MM, DM | 45 to 69 | 2 years | 211,922 | 67.50% |
| Norway | 1996 | DM | 50 to 69 | NA | 199,818 | 76.00% |
| Poland | 2006 | MM, DM | 50 to 69 | NA | 985,364 | 39.00% |
| Portugal (Central Region) | 1990 | DM | 45 to 69 | 2 years | 100,348 | 63.00% |
| Portugal (Alentejo Region) | 1997 | DM | 45 to 69 | 2 years | 7298 | Data not available |
| Saudi Arabia | 2007 | | 40 to 64 | | 6200 | 19.00% |
| Spain (Catalonia) | 1995 | MM, DM | 50 to 69 | NA | 527,000 | Data not available |
| Spain (Navarra) | 1990 | DM | 45 to 69 | 2 years | 40,016 | 87.30% |
| Sweden | 1986 | MM, DM | 40 to 74 | 18 months | 1,414,000 | 70.00% |
| Switzerland | 1999 | MM, DM | 50 to 69 | NA | 60,700 | 48.20% |
| United Kingdom | 1988 | MM, DM | 50 to 69 | | 1,957,124 | 73.30% |
| United States | 1995 | MM, DM, CBE | 40 to 75+ | 1 to 2 years | 416,000 | 66.50% |
| Uruguay | 1990 | MM, CBE, U, BSE | 40 to 69 | 2 years | 352,000 | Data not available |

Note: Data are from a survey of International Cancer Screening Network (ICSN) country representatives, conducted in 2012.⁷⁶ MM, screen-film mammography; DM, digital mammography; CBE, clinical breast exam; BSE, breast self-examination; U, ultrasound.

outcome prediction, where the therapy is limited to a very short time span due to the commonly advanced nature of the breast-invasive tumor. The physician needs confirmation that the chosen chemotherapeutics are effective in shrinking the tumor volume or affecting its metabolism already after one or two cycles. As spatial resolution is secondary and the overall tumor response is desired, a low spatial resolution technique yet nevertheless with high contrast to changing oxygen consumption or vascularity can suffice.

Similarly to diagnostic technologies, therapeutic approaches show a significant qualitative difference between high- and middle-income countries on the one hand and low-income countries on the other hand. It is particularly evident in the latter group where the changing population age-pyramid coincides with rapidly changing environmental exposure. Middle-income countries try to emulate high income countries in their approach to treat advanced BC, which comprises neoadjuvant chemotherapy, surgery, intensity modulated radiation therapy, and chemotherapy with tyrosine or aromatase inhibitors. These treatment approaches pose a tremendous strain on the health care systems of middle-income countries, and they are generally not affordable for low-income countries. Hence, the majority of the women in low-income countries are not offered therapy, which is often further enhanced by a stigma with which these women are associated due to a BC diagnosis.

Hence, there are plenty of opportunities for novel enabling technologies to fundamentally change the clinical management of BC in high-income countries as well as low- and middle-income countries, so the technologies introduced into these markets will be different.

4.2 Optical Technologies Aimed at Improving BC Risk Assessment, Diagnostics, and Response Prediction

Various demographic- and lifestyle-based BC risk assessment tools have been developed, such as the Gail breast cancer risk assessment model or familiar risk models,^{77,78} and shown to be of utility for some screening decision making. However, their predictive power or odds ratio hovers below 2, and hence, they are not of utility to adjust entry and frequency of standard screening programs for the entire female population. An additional significant impediment of these risk assessment techniques is that some required predictors are not available until women are of standard mammographic screening age, missing the population of the sub-40- to 50-year-old women.

Risk assessment based on physical risk factors, analogous to blood pressure measurements for cardiovascular, cancer, and other diseases, does not face these limitations. To this effect, there is ample research showing that mammographic breast density (MBD) is one of the strongest risk factors, reaching odds ratios of up to 6 for two-dimensional mammographic projections when evaluating the top 25th percentile versus the lowest 10th percentile.⁷⁹ For 3-D assessment of the mammographic density, odds ratios up to 10 are anticipated, which suggest a causal relationship between MBD and BC.⁸⁰ When considering personalized oncology, the use of MBD has not progressed beyond recommendations to reduce the screening frequency for women with low MBD, so MBD is not suitable as a criterion for entry into a standard screening program. MBD cannot overcome the limited access to BC screening programs in low- and middle-income countries and as such does not overcome one of the major bottlenecks in BC management worldwide.

The risk assessment for a prescreening technology to be of utility in BC management in high-income countries needs to provide extremely high sensitivity comparable to mammography for the equivalent MBD and good specificity, as this is only a prescreening technology and the screening entry and frequency are to be personalized. In settings with limited access to standard screening technology, the main obligations are to identify the appropriate fraction of the population to advance to mammographic screening, thus optimizing the infrastructures for the women at highest risk. If the instrument is affordable, it can be shown that such a program is financially self-sustaining. For example, reducing the stage III/IV tumor incidence in countries with population of >100 million from the mid-30% to <15%, entirely attainable when the available infrastructure approximates the OECD guidelines of 12 mammographs per 1 million BC cases, treatment costs can be reduced by over 300 to 500 million USD/year depending on the actual population size and the female life expectancy. Optical prescreening (Fig. 5) would be built on the intrinsic breast tissue optical properties using either absorption⁸¹ or fluorescence properties⁸² or both,⁸³ or on optical coherence spectroscopy.⁸⁴

Here, in particular, the work of the Turino^{85,86} and Toronto^{81,87-89} groups have demonstrated the ability to identify women with known physical risk factors, such as MBD^{79,90,91} or biological event linked to the development of breast cancer, such as glandular atrophy during perimenopause and postmenopause.⁹² While it is not clear at this time what fraction of the BC can be attributed to these different risk factors, however, the differences in the breast composition are accessible optically. Contrast is provided by the wavelength-dependent absorption spectra of predominantly water, lipid, hemoglobins, and collagen as well as by changes in the light scattering coefficients. The risk to develop BC does not correlate with particular tissue substructures, and hence spatial resolution is not required. The Toronto group favors steady-state spectrally resolved diffuse reflectance measurements, using either only chemometric analysis, such as principal component analysis, for disease classification^{93,94} or quantitative tissue chromophore extraction building on prior work by Farrell et al.⁹⁵ to first extract the spectral absorption and scattering coefficient followed by least-square fitting to derive the chromophore concentrations. The Milano group favored the use of time domain measurements to extract chromophore concentrations, allowing an analytical determination of the spectrally resolved light transport parameters preferable in establishing relationships of optical properties and known BC risk factors and future incidence of BC.

The ability to identify women with high MBD has been demonstrated for a screening aged population with sensitivity and specificity >0.9 when combining with menopausal status and body mass index by the Toronto group⁹⁶⁻⁹⁸ and a $p < 0.0001$ to differentiate a BIRADS 4 scores indicative for high MBD versus lower BIRADS scores by the Milano group.^{85,86} Strong correlations have also been demonstrated for other risk factors, such as parity, age, and menopausal status.^{87,89}

For immediate application in low- and middle-income countries, robust and low-cost solutions, possibly based on cw measurements, are preferable as long as they satisfy the sensitivity and specificity requirements in identifying the subpopulation at highest risk to benefit from the screening infrastructure. High sensitivity and specificity >0.8, sufficient to be subsequently screened by butting national screening programs,

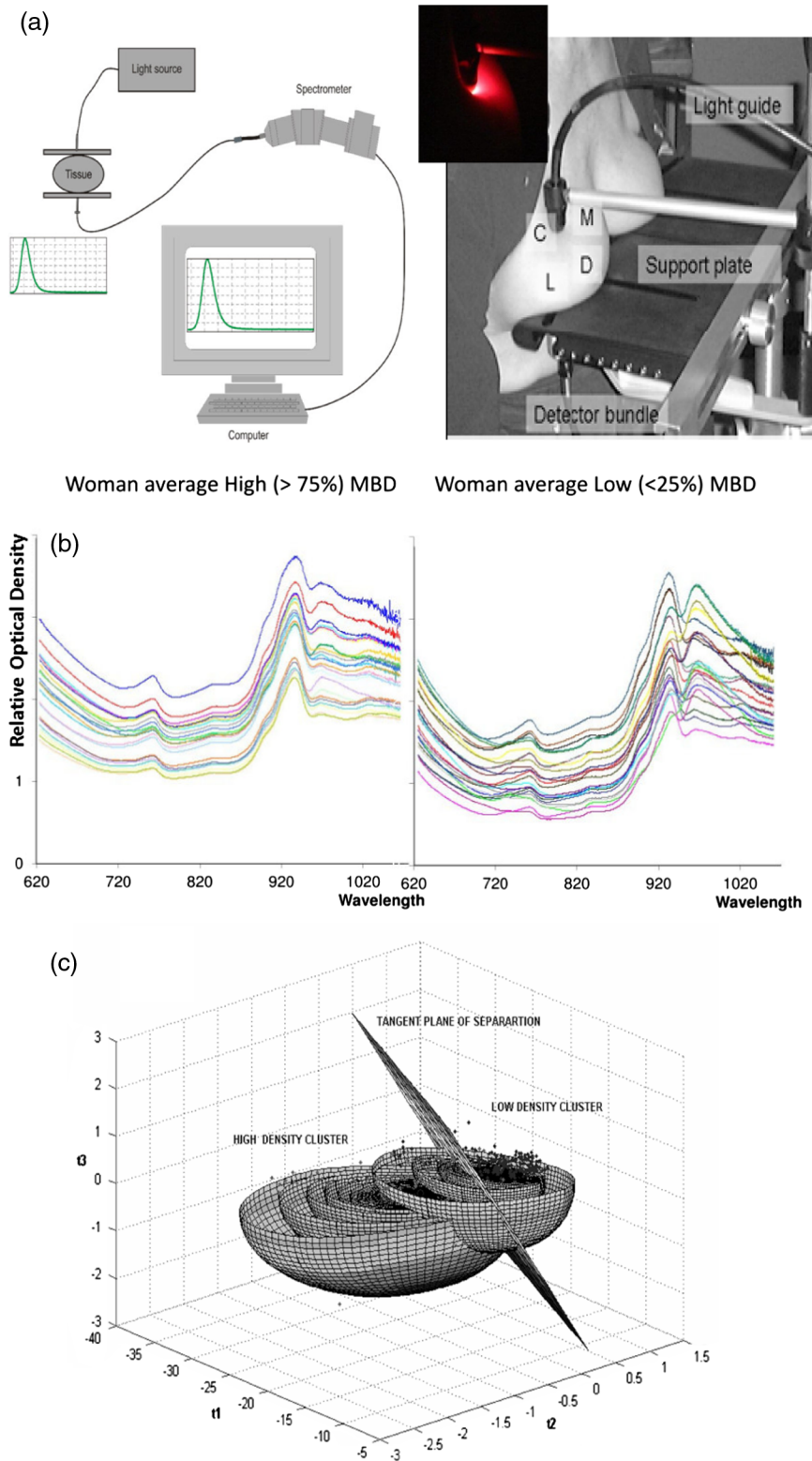


Fig. 5 (a) Principal optical components for transmission measurements (left) and setup with four quadrants identified on the right breast (right). The small insert shows the tissue during measurements. (b) Optical density (OD) per physical optode separation (or relative optical density) in units of 1/cm for women with high (left) and low (right) mammographic breast density (MBD), respectively. (c) Chemometrix (principal component analysis) score based clustering of high MBD and low MBD.

can be achieved only using relative spectra shape, and thus, absolute instrument calibration is not required, facilitating the use of these instruments in resource-limited environments.

Optical tools are also being investigated to predict treatment response, in particular, for neoadjuvant chemotherapy, during the initial work therapeutic session to determine if a particular chosen treatment regime has the desired effect toward shrinking of the tumor to render it amenable to therapy. In particular, frequency domain spectroscopic scanning or tomographic approaches are being developed by various groups.^{99–107} However, frequency domain optical tomography has demonstrated only limited utility as a screening tool due to its limited spatial resolution,¹⁰⁸ even when using a large number of source and detector pairs. Using added information, such as spatial information about the distribution of fatty versus glandular tissue from clinical imaging and knowledge of the chromophores' absorption spectra demonstrated,^{109–111} does not significantly improve the resulting spatial resolution in order to detect early-stage cancers at a rate comparable to current clinical imaging technologies even in premenopausal women. While some of the technology is comparable to that described previously for risk assessment, the number of source-detector pairs is commonly larger to achieve some spatial localization of the contrast. As vascular normalization is a primary goal of neoadjuvant chemotherapy, pruning of the aberrant vascular tree will modify the total hemoglobin concentration as well as the oxygen saturation in the affected tissue volumes.^{106,112} During initial clinical studies, it was demonstrated that correct response prediction was achieved and that the hemoglobin contrast to normal tissues exceeds a ratio of 2.

Photoacoustic imaging, as for example developed by the Twente group with their photoacoustic mammography,¹¹³ is promising as a screening alternative, particularly for premenopausal women where tumors are masked by high mammographic density as shown in a comparative study versus MRI.¹¹⁴ Contrast is relying on the angiogenesis associated with tumor development for the selective absorption contrast. As absorption is mostly independent of the structures, providing high MBD photoacoustic mammography is also applicable in premenopausal women. In a recent small clinical study, Kitai et al. demonstrated the ability to detect all cases of ductal carcinoma *in situ* and most tumors that underwent prior neoadjuvant chemotherapy.¹¹⁵

The lower technical complexity of photoacoustic imaging over diffuse optical tomography makes it possibly the preferred technology independent of the available health care resources.

To summarize opportunities in the management of BC, the field of risk assessment or prescreening has significant potential particularly for younger women at risk. Here photonics-based diagnostics may complement US- or MRI-based assessment and/or preselection of women at risk of developing or harbouring BC in a resource-limited environment. Photoacoustic imaging can also become a valuable tool for BC detection, whereby monitoring of neoadjuvant chemotherapy by diffuse optical tomography should be considered whenever this therapy is offered.

4.3 Photonics-Based Therapeutic Solution

As mentioned previously, there is indirect evidence that the current decrease in BC-related mortality in high-income countries is predominantly due to improved therapeutic efficacy and the present move towards personalized cancer medicine. The number of targets for BC is constantly increasing ranging from

tyrosine and protein kinase inhibitors, epigenetic regulations, and nanomedicine with several of these approaches being introduced particularly in high-income countries. However, independent of the various therapies offered to the patient, surgical removal of the primary tumor is the standard of care, and its efficacy is limited by the need to demonstrate tumor-free resection margins. In a simplification to the use of FGR of brain tumors described previously, in BC, significant wider resection margins are acceptable,¹¹⁶ reducing the need for quantitative assessment of fluorescence. In general, the aim is a move towards near-infrared fluorescence in order to capture nests of infiltrating tumors several millimeters below the resection cavity surface.^{117,118} Clinical trials for indocyanine green (ICG) fluorescence are ongoing, so primary data have not been published¹¹⁹ to date.

A second clinical application for fluorescence guidance is the intraoperative detection of sentinel lymph nodes using ICG as contrast medium^{120,121} with or without active targeting, or intensely staining blue dyes. The first published multicenter clinical trial¹²² demonstrated an equal detection ability compared to radiolabeling or blue dyes. This was also confirmed by a recent meta-analysis¹²³ suggesting equal performance between fluorescence and radiolabel detection.

An alternative to surgical removal of the primary tumor was evaluated using either PDT^{124,125} or photothermal applications, such as with interstitial laser photocoagulation^{32,126–128} and interstitial laser hyperthermia.^{129,130} Particularly the photothermal ablation models are currently not being researched as it becomes increasingly evident that complete surgical resection or ablation of the primary tumor will lead to high five-year survival rates, but without an immune effect introduced, a long-term survival is not guaranteed.¹³¹ More recent research is focusing on the therapy of metastatic BC particularly with spinal and bone involvement.¹³²

An interesting photon generation solution was proposed by Batista and Liang using solar irradiation, which could potentially have utility in extreme resource-limited environments when the primary tumor is to be destroyed *in situ*.¹³³

In summary, particularly supporting surgical lumpectomy by fluorescence-guided resection and detection of tumor infiltrated lymph nodes currently appear to be the most promising avenues for photonics solutions in the management of BC. Removal of the primary tumor is currently still best achieved with surgical resection followed by the various chemotherapies and radiation therapies aimed at treating the remaining micro metastasis and preferably also inducing the desired immune response.

5 Treatment of Hyperplastic Nasal Turbinates

Inferior turbinate hypertrophy is a common cause of nasal airway obstruction. Patients that are refractory to conservative pharmacological treatment require surgery, often accompanied with long-term bleeding and further discomfort. Surgical techniques including total or partial turbinectomy, laser surgery, electrocautery, cryosurgery, and radiofrequency ablation are available.¹³⁴ Endonasal laser treatments cause limited side effects with little or no bleeding while similar tissue reduction could be obtained, thus reaching high patient acceptance.^{135–138} Since the early 1980s, various types of laser systems have been developed for surgical endonasal applications. Systems for clinical applications include the CO₂, Nd:YAG, Ho:YAG, KTP, as well as diode lasers of different wavelengths.¹³⁹ Generally, different laser parameters (power, energy) and application

modalities (contact, noncontact, interstitial, superficial) were used.¹³⁹

Dependent on the laser wavelength and the associated different optical parameters of the tissue, the light-tissue interaction varies in terms of amount of coagulation and ablation volumes. Most of the commonly available diode laser systems provide light at wavelengths of $\lambda = 800$ to 1000 nm, mainly causing coagulative tissue effects when applied in noncontact mode. In comparison to CO₂ and Nd:YAG lasers, diode lasers have lower acquisition and maintenance costs and are more versatile in the clinical setting due to their smaller size. Recently, laser systems emitting in the spectral region between $\lambda = 1300$ and 2100 nm became clinically available and were tested for this application.

5.1 Endonasal Laser Treatment

After topical anesthesia [e.g., 4% tetracaine and 0.5% xylocaine solution (1:1), 10 to 15 min] photo- or video-documentation via a rigid endoscope should first be performed. Prior to introduction of the laser light application system, laser safety precautions are mandatory. Conveniently, laser light should be applied in noncontact mode using a flexible silica bare fiber (core diameter: 400 to 600 μm) guided via a device for precise endonasal fiber guidance.¹⁴⁰ Laser parameters setting need to be adjusted with respect to the laser emission wavelength [e.g., 8 to 12 W for 940 nm,^{141,142} 4 to 5 W for 1470 nm,¹⁴¹⁻¹⁴³ 2 to 4 W for 1940 nm.¹⁴⁴ So far, diode lasers emitting at 900 to 1000 nm are in clinical use. Maneuvers for energy application itself should be performed via guiding the fiber from the posterior to the anterior free edge of the inferior turbinate under endoscopic control until adequate blanching of the tissue is obtained as judged by the operating surgeon. In cases where the head of the inferior turbinate appeared to be especially prominent, only some single laser spots were directed onto the head of the turbinate. Postoperatively, nasal cavities were treated with antibiotic and steroid-containing ointment (e.g., Jellin-Neomycin®: 0.25 g fluocinolone acetonide / 4.25 g neomycin sulfate). Patients received prescriptions for nasal ointments and nasal decongestants.

A typical outpatient laser-assisted inferior turbinate reduction of the hyperplastic inferior turbinate using a Tm:fiber laser emitting at 1940 nm at 3 W using a fiber guidance system is shown in Fig. 6, prior to, immediately after, and two months after treatment.¹⁴⁴

5.2 Clinical outcome of Endonasal Laser Treatment Studies

Investigations and clinical trials show the safety and efficacy of laser treatment for volume reduction of hyperplastic turbinates in single cases as well as in prospective, randomized, and blind studies. The macroscopically visible tissue effect depends on the wavelength used. Observations by the operating surgeon on the basis of tissue whitening and tissue reduction confirm that 1940 and 1470 nm irradiation was about equivalent to the effects of the commonly used 940 nm laser system, yet it required a reduced irradiance, a significantly shorter treatment time, and less total energy.¹⁴¹⁻¹⁴³ These treatment procedures could be performed as an outpatient procedure under local anesthesia, and therefore, the patient acceptance and satisfaction were exceptionally high. The overall pain sensation was very moderate, with a trend towards less intraoperative pain using the longer wavelengths.¹⁴¹ Neither minor nor major complications could be witnessed in these studies during operation as well as postoperatively.¹⁴⁵⁻¹⁴⁷ The main symptoms due to hyperplastic inferior turbinate (nasal congestion and nasal obstruction during exertion) could be significantly improved. Correspondingly, a significant symptom improvement was also shown in the validated assessment tool SNOT 20 GAV (“need to blow nose”).^{141,144}

Especially the long-term outcome seems to be the critical issue with the laser treatments of the turbinates.^{139,148-153} Moreover, there is currently no clear consensus or gold standard in the literature indicating the most optimal technique for turbinate reduction.^{139,154-157} This lack of a gold standard renders an appropriate evaluation or a comparison of novel techniques challenging. Nevertheless, laser-assisted and radiofrequency-assisted reduction of hyperplastic turbinates seem to be standing out as methods that can be applied under local anesthesia providing minimal morbidity.¹³⁹ For these reasons, the 940 nm diode laser was used for more than a decade for this indication and is regarded as the standard laser application.^{139,145,146,152}

With regard to lowering the applied irradiation, medical devices emitting at 1940 nm should be preferred, but these are rarely available in hospitals. As the 1470 nm diode laser systems are more widespread, these systems offer a highly efficient alternative to conventional diode laser systems in treatment of nasal obstruction due to hyperplastic nasal turbinates. In therapy-refractory rhinitis medicamentosa, outpatient diode laser inferior turbinate reduction of hyperplastic inferior turbinate represents

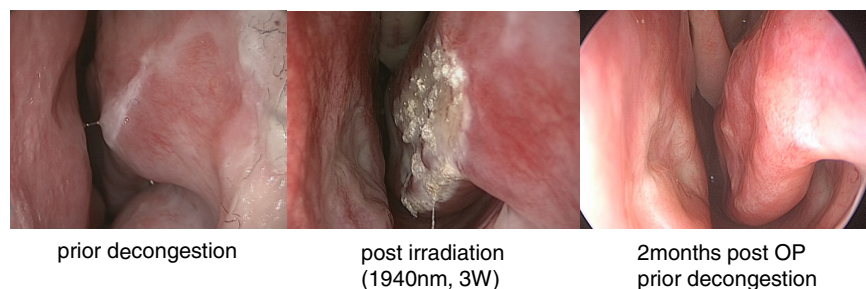


Fig. 6 Outpatient therapy for laser-assisted inferior turbinate reduction of a hyperplastic inferior turbinate using a Tm:fiber laser emitting at 1940 nm at 3 W using a fiber guidance system.¹⁴⁴ (a) Endonasal situation prior to laser energy application without decongestion showing the turbinate hindering continuous airflow, (b) immediately after laser energy application coagulation could be observed, and (c) two months after laser treatment the reduction of the turbinate is obvious (without decongestion) and continuous airflow is possible.

a highly effective, safe, and well-tolerated treatment option that provides long-lasting recovery by markedly improving nasal airflow and stopping addiction to nasal decongestants.¹⁵⁸ It had also been shown that rhinomanometry with topical decongestion has a high predictive value for the objective outcome of laser-assisted turbino-plasty.¹⁵⁹

In conclusion, laser surgery of inferior turbinates can be performed as an outpatient procedure under local anesthesia. Due to a minimally invasive and controllable coagulation and ablation of soft tissue, almost no complications or bleedings were observed during the operation or postoperatively. Depending on the chosen parameters (power, energy) and the application modalities, laser treatment of hyperplastic inferior nasal turbinates achieved comparable or better results than most of the conventional techniques for turbinate surgery, like conchotomy, electrocautery, cryotherapy, chemical cauterization, and vidian neurectomy. Laser treatment can be considered a useful, cost-effective, and time-saving procedure for the reduction of hyperplastic inferior nasal turbinates. Short operation time, good clinical outcome, and minor side effects compared to other surgical methods provide an excellent clinical response of the patients.

6 Endovenous Laser Treatment of Varicose Veins

Varicose veins are widened vessels due to weakened connective tissue and insufficiency of vein valves. In middle Europe, the incidence is ~50% (age: 20 to 75) with a female / male ratio of 2 / 1). Located on the lower extremities, the symptoms are subjectively described as sensations, such as heavy legs, tension, swelling, pain while standing and sitting, discoloring, and phlebitis. The involved structures are mainly the *vena saphena magna* (VSM) and the *vena saphena parva*. In half of the cases, patients need surgical intervention with the main goal of complete destruction of the vessel. Besides methods of conservative surgery and stripping treatments during the last 15 years, endoluminal procedures like sclero-therapy, radio-frequency ablation, and endovenous laser therapy (ELT) have gained attention among the medical community. Figure 7(a) shows the principle of a clinical ELT treatment of the VSM of a right leg. Typically, the physician pulls the fiber backward at a velocity of 1 mm/s while the assistant is imaging the endoluminal location of the fiber by means of US. By means of US, the laser energy induced thermal effects can also be visualized as shown in Fig. 7(b).

The first clinical results of ELT were published in the beginning of this millennium.^{160,161} The endothermal damage of the vein wall arises from thermal shrinkage of connective tissue and thermal denaturation by coagulation induced shrinkage of the lumen and consecutive occlusion of the treated vein.^{162–168} The clinical outcome looks very promising. Meta-analytic studies give evidence that these innovative techniques result in a similar clinical outcome as conventional surgical stripping.^{169–175} Currently the laser medical equipment is still under development. One disadvantageous characteristic of ELT is the broad spectrum of different treatment protocols using a variety of laser systems and devices for endovenous application. Recently, systematic experimental investigations and analyses of clinical results have increased the knowledge of the relation between particular details of endovenous laser application and clinical results.^{162,165,168,176}

Due to the diversity of laser parameters (e.g., wavelength, light application system, power, irradiance, irradiation) and

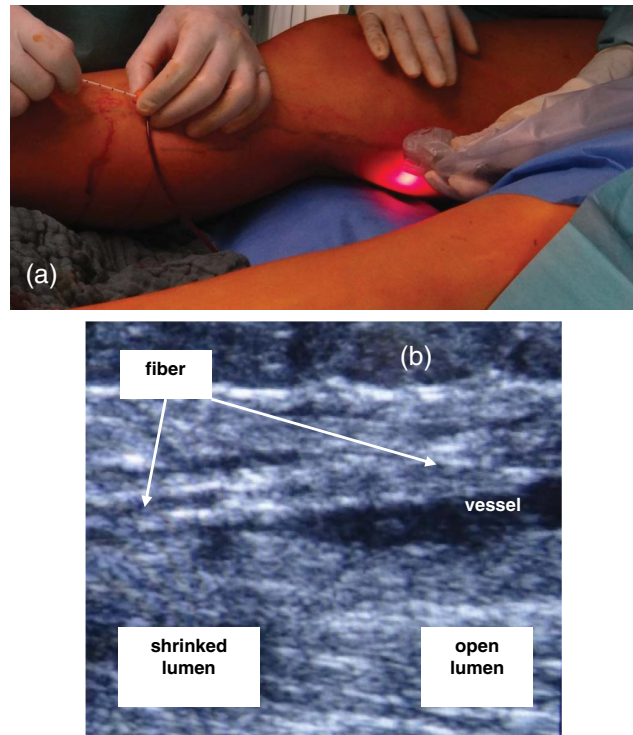


Fig. 7 (a) Clinical situation for endovenous laser therapy treatment of *vena saphena magna* of a right leg. Veins and perforators are marked in black on the skin. The medical doctor (left two hands) pulls the fiber backwards at a velocity of 1 mm/s. The assistant (right two hands) positions the ultrasound (US) head to image the endoluminal location of the fiber (red light transmission of the pilot beam through the skin is obvious). (b) US image of the location and the state of the vein. In the left part, the vein lumen is closed by thermal shrinkage while the fiber is still in the lumen. In the right part, the lumen is still not affected by laser energy; thus, the lumen is widened.

the corresponding variable interaction with the target tissue, physicians request for a precise, reproducible, safe, standardized procedure and treatment protocol,^{177–180} which includes the strategic investigation of light application systems^{168,176,181} as well as potential on-line feedback.

6.1 Endovenous Light Application

The endovenous laser treatment relies on the transformation of luminous energy into heat due to absorption. This process depends on the wavelength-dependent optical properties of the tissue and can be investigated by MC simulations.^{182–185} Thus, the endoluminal application of laser energy implies the necessity of controlling a variety of parameters all together influencing the alteration produced on the vein wall. Variations in the laser wavelength, power settings, and irradiance result in different temperature levels and thermal alterations up to perforation.^{182,183,186–188} As blood is the primary medium around the laser fiber tip, it influences the mechanism and the alteration process as well, especially in cases where carbonization is induced.^{162,164,181,189}

Initially, laser energy was applied by using bare fibers emitting coaxially in the vessel lumen. The approach was the development of a specific radial emitting fiber to deliver the energy in direction to the vessels wall.^{167,168,176,190} In dependency of the used wavelength, the transmission through the existing thin

blood layer around the fiber tip differs. As shown in Fig. 8, irradiation pattern showed maximum intensity deflected in an angle of ~ 70 deg without any axial irradiance transmission. The measured transmission efficiency of such device was 94 to 97%. In comparison to the bare fiber technique, the irradiance (if contact to the tissue is assumed) can be reduced by a factor of 7 to reach irradiance values just below the ablation threshold of tissue.^{168,176}

In tests of the radial fiber technique on an *ex vivo* vein model¹⁶⁷ using heparinised blood containing veins, a shrinkage in length, a thickening of the wall, and the increased rigidity assessed by digital inspection could be achieved perfectly without any perforation.^{167,168,176,190} Additional investigation of the wavelength dependency of this treatment also showed that using a laser emitting at 980 nm an output power of $P_{980} = (20 \pm 2)$ W is needed to achieve the desired macroscopic tissue alteration. In contrast, for a 1470 nm emitting diode laser, an output power of $P_{1470} = 6$ to 8 W is only necessary to achieve the same macroscopic results. On inspection of the surgically opened lumen of the vein, charred blood clots could be observed in the case of 980 nm irradiation, whereas in case of 1470 nm irradiation, a clean white coagulated vein intima surface was observed.^{167,168,190} Further investigation also showed wavelength-dependent discrepancies.^{186,191} These effects are clearly related to the wavelength-dependent optical properties of vein tissue and blood¹⁸⁹ and were confirmed by MC simulations.^{182–185}

Heat induction ($T = 85^\circ\text{C}$ for 30 s) of the vein tissue samples showed a swelling of the sample concomitant with shrinkage in length. Additionally, the reddish vein color changed to whitish color of denatured tissue. The feeling sensation changed from flexible, smooth, and elastic to rigid and “macaroni-al-dente-like.” Vein tensile experiments showed native veins are elastic and can be stretched with low tensile power up to rupture, while cooked veins are inelastic and high tension powers are necessary for rupture. Both factors may explain patients’ description of having stretch discomfort after ELT.^{167,168,190}

Technologies such as the 360 deg radial fiber in combination with 1470 nm laser light^{168,192} look promising as a means to induce safe, reliable, and reproducible tissue alteration for the ELT. By means of these optimizations, ELT treatment is getting

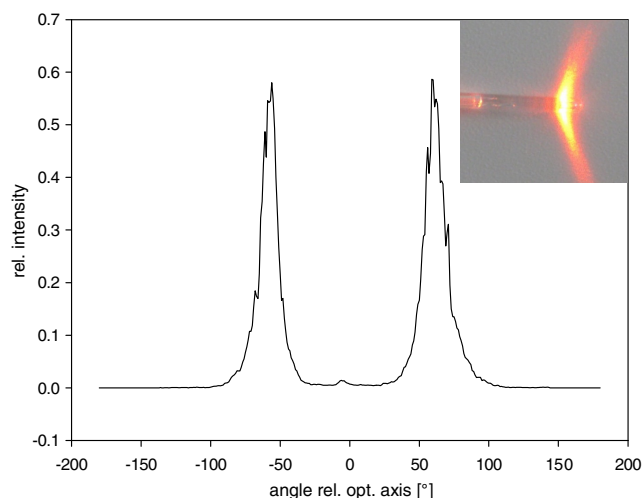


Fig. 8 Radially emitting fiber and its irradiation characteristics.

closer to the goal of standardizing an effective method for the treatment of varicose veins. In a variety of investigations, disadvantages of previous ELT application techniques could be shown.^{168,187,188} The introduction of the more effective wavelength and the new radial procedure has been established in clinical use since 2009.^{193,194} First clinical studies show a clinical benefit.^{195–200} Today, long-term follow-ups confirm the persistent effectiveness and safe occlusion of the veins.²⁰¹ Based on the reduction of undesirable side effects and the accelerated convalescence, endovenous treatment methods became the treatment option of first choice for insufficient veins in some countries.^{202,203} Despite these improvements, some minor effects like carbonization and adhesion of the fiber to the vessels wall could still be observed during the clinical procedure. Therefore, implementation of feedback technologies may further assist standardization of the procedure.

6.2 On-Line Monitoring During ELT

Although endoluminal techniques are medically approved and the clinical outcome of endoluminal treatments are accepted by physicians, due to meta-analysis of a large cohort studies,^{204–210} as well as by the patients there are still requests for further improvement as adjacent structures should be prevented from temperature-related changes. Currently, real-time monitoring of physical, physiological, and tissue conditions is not available. Feedback information may have the potential of controlling the treatment or supplying immediate hints for the success of the treatment.

Tissue effects that could be optically detected in principle are shrinkage of the lumen, white light remission of the vessel wall, autofluorescence of the vessels wall, and temperature on the tissue or at the fiber tip. Investigations were performed to develop systems for endoluminal *in vivo* on-line monitoring of such parameter, during laser energy application and within the irradiation field.^{176,211}

MC simulation of optical detection of the shrinkage effect looks promising only for small vessel calibres. Using the radially emitted light of wavelengths between 600 nm (pilot beam) and 1500 nm (therapeutic wavelength), which is reflected by the vessels wall and then detected by the same fiber, showed that the moving vessel wall can only be detected when the distance between the fiber and tissue is < 2 mm in case of being filled with pure water and < 1 mm in case of the presence of blood. As native and coagulated vein tissues differ in their optical properties, the white light remission spectrum changes its shape during the denaturation process accordingly. Unfortunately, in the presence of blood, white light remission measurements as well as *in situ* measurements of autofluorescence are challenging. Finally, a temperature measuring system based on the analysis of the temperature-dependent fluorescence of a ruby crystal is developed.²¹¹ This sensor can be manufactured such that it is inert and biocompatible. It was tested to be useable in a high electromagnetic field, such as within the laser light irradiation field. Temperatures ranging from 20 to 200°C could be measured with an accuracy of $\pm 2^\circ\text{C}$. Clinically adapted *ex vivo* experiments in a blood filled vein showed accurate measurements when the sensor tip is positioned in the vein parallel to and directly within the radially-emitting therapeutic fiber.²¹¹

In conclusion, the suggested technical feedback improvements are not yet clinically available. As visual control of the immediate tissue effect, such as lumen shrinkage or vein wall thickening, extra corporal UA and photoacoustic

techniques are suggested but used from the skin surface. Additionally, the control of the pullback velocity of the treatment fiber and the irradiation parameters may yield improved light dosimetry. Implementation of a local endoluminal temperature may yield an improved reliable and successful treatment for the benefit of the patient.

7 Conclusion

Research and development in laser medicine and biophotonics is very dynamic and continuously expanding. National and international presentations induce critical discussions between members of the scientific and medical communities. These sessions are key opportunities and are highly necessary to identify and explore unmet clinical needs and detailed requests from clinicians. The incorporation of technicians and companies is indispensable to support the development of prototypes and to start clinical trials. Unfortunately, only after clinical testing, sometimes in comparison to established nonoptical clinical procedures, the impact of new biophotonic technologies on clinical application becomes obvious, in a positive or negative way. This constitutes one example of a multiplicity of barriers that need to be conquered before achieving clinical application and, finally, full acceptance in the medical community. The collection of conference-related references cited in this article may indicate that long-term highly motivated research and development is necessary to reach clinical success. Furthermore, the presented examples clearly show that knowledge about the requirements of physicians in their clinical work is the basis for beneficial technical developments. The transfer of scientific knowledge into components and systems with either new or improved properties may then allow researchers to create new innovative tools to support clinicians in their clinical practice.

Acknowledgments

The authors would like to thank all coworkers, technicians, and students who took part in the diverse projects as each and every single experiment and scientific discussion that resulted in improvements to bring new laser-based biophotonic concepts into clinical reality. The authors would also like to thank the companies for their long-term support with devices and equipment to enable the teams to perform the clinical-related research. Finally, all our sponsors and grant providers are acknowledged for financially supporting the numerous projects. There are many more examples and techniques in a variety of medical disciplines that could also be mentioned. The authors apologize for only giving insight into a small selection of successful approaches chosen from their own points of view and experiences.

References

- G. Hennig et al., "Dual-wavelength excitation for fluorescence-based quantification of zinc protoporphyrin IX and protoporphyrin IX in whole blood," *J. Biophotonics* **7**(7), 514–524 (2014).
- G. Hennig et al., "Dual-wavelength excitation to reduce background fluorescence for fluorescence spectroscopic quantitation of erythrocyte zinc protoporphyrin-IX and protoporphyrin-IX from whole blood and oral mucosa," *Proc. SPIE* **8951**, 89510J (2014).
- M. B. Zimmermann and R. F. Hurrell, "Nutritional iron deficiency," *Lancet* **370**(9586), 511–520 (2007).
- J. M. Tielsch et al., "Effect of routine prophylactic supplementation with iron and folic acid on preschool child mortality in southern Nepal: community-based, cluster-randomised, placebo-controlled trial," *Lancet* **367**(9505), 144–152 (2006).
- S. Sazawal et al., "Effects of routine prophylactic supplementation with iron and folic acid on admission to hospital and mortality in preschool children in a high malaria transmission setting: community-based, randomised, placebo-controlled trial," *Lancet* **367**(9505), 133–143 (2006).
- WHO, "Conclusions and recommendations of the WHO Consultation on prevention and control of iron deficiency in infants and young children in malaria-endemic areas," *Food Nutr. Bull.* **28**(4 Suppl), S621–627 (2007).
- M. B. Zimmermann, "Methods to assess iron and iodine status," *Br. J. Nutr.* **99**(Suppl 3), S2–9 (2008).
- F. K. Grant et al., "Comparison of indicators of iron deficiency in Kenyan children," *Am. J. Clin. Nutr.* **95**(5), 1231–1237 (2012).
- P. Suominen et al., "Serum transferrin receptor and transferrin receptor-ferritin index identify healthy subjects with subclinical iron deficits," *Blood* **92**(8), 2934–2939 (1998).
- C. Thomas and L. Thomas, "Biochemical markers and hematologic indices in the diagnosis of functional iron deficiency," *Clin. Chem.* **48**(7), 1066–1076 (2002).
- A. A. Lamola and T. Yamane, "Zinc protoporphyrin in the erythrocytes of patients with lead intoxication and iron deficiency anemia," *Science* **186**(4167), 936–938 (1974).
- R. F. Labbe, H. J. Vreman, and D. K. Stevenson, "Zinc protoporphyrin: a metabolite with a mission," *Clin. Chem.* **45**(12), 2060–2072 (1999).
- E. Rossi and P. Garcia-Webb, "Red cell zinc protoporphyrin and protoporphyrin by HPLC with fluorescence detection," *Biomed. Chromatogr.* **1**(4), 163–168 (1986).
- B. Kaul, G. Slavin, and B. Davidow, "Free erythrocyte protoporphyrin and zinc protoporphyrin measurements compared as primary screening methods for detection of lead poisoning," *Clin. Chem.* **29**(8), 1467–1470 (1983).
- G. Metzgeroth et al., "Zinc protoporphyrin, a useful parameter to address hyperferritinemia," *Ann. Hematol.* **86**(5), 363–368 (2007).
- J. Hastka et al., "Washing erythrocytes to remove interferents in measurements of zinc protoporphyrin by front-face hematofluorometry," *Clin. Chem.* **38**(11), 2184–2189 (1992).
- J. Hastka et al., "Zinc protoporphyrin in anemia of chronic disorders," *Blood* **81**(5), 1200–1204 (1993).
- K. H. Yu, "Effectiveness of zinc protoporphyrin/heme ratio for screening iron deficiency in preschool-aged children," *Nutr. Res. Pract.* **5**(1), 40–45 (2011).
- "Zinc-protoporphyrin/protoporphyrin HPLC kit: manual (preliminary)," 2011, http://www.immundiagnostik.com/fileadmin/pdf/Zink-Protoporphyrin_KC2700.pdf.
- W. E. Blumberg et al., "The hematofluorometer," *Clin. Chem.* **23**(2), 270–274 (1977).
- R. E. Hirsch, M. J. Lin, and C. M. Park, "Interaction of zinc protoporphyrin with intact oxyhemoglobin," *Biochemistry* **28**(4), 1851–1855 (1989).
- R. J. Stoltzfus et al., "Iron supplementation of young children: learning from the new evidence," *Food Nutr. Bull.* **28**(4 Suppl), S572–584 (2007).
- E. Buhmann, W. C. Mentzer, and B. H. Lubin, "The influence of plasma bilirubin on zinc protoporphyrin measurement by a hematofluorimeter," *J. Lab. Clin. Med.* **91**(4), 710–716 (1978).
- P. Granjean and J. Lintrup, "Sources of variation in fluorometry of zinc protoporphyrin in blood," *Scand. J. Work Environ. Health* **7**(4), 311–312 (1981).
- R. F. Labbe, A. Dewanji, and K. McLaughlin, "Observations on the zinc protoporphyrin/heme ratio in whole blood," *Clin. Chem.* **45**(1), 146–148 (1999).
- R. Gorodetsky et al., "Direct fluorometric determination of erythrocyte free and zinc protoporphyrins in health and disease," *Clin. Biochem.* **18**(6), 362–368 (1985).
- R. B. Schiffman and P. R. Finley, "Measurement of near-normal concentrations of erythrocyte protoporphyrin with the hematofluorometer: influence of plasma on 'front-surface illumination' assay," *Clin. Chem.* **27**(1), 153–156 (1981).
- G. Hennig et al., "Bandwidth-variable tunable optical filter unit for illumination and spectral imaging systems using thin-film optical band-pass filters," *Rev. Sci. Instrum.* **84**(4), 043113 (2013).
- I. Pavlova et al., "Monte Carlo model to describe depth selective fluorescence spectra of epithelial tissue: applications for diagnosis of oral precancer," *J. Biomed. Opt.* **13**(6), 064012 (2008).

30. CBTRUS, "CBTRUS statistical report: primary brain and central nervous system tumors diagnosed in the United States in 2004-2007," 2011, www.cbtrus.org.
31. M. L. Siker et al., "Age as an independent prognostic factor in patients with glioblastoma: a Radiation Therapy Oncology Group and American College of Surgeons National Cancer Data Base comparison," *J. Neurooncol.* **104**(1), 351-356 (2011).
32. J. D. Voigt and M. Torchia, "Laser interstitial thermal therapy with and without MRI guidance for treatment of brain neoplasms: a systematic review of the literature," *Photonics Lasers Med.* **3**(2), 77 (2014).
33. T. R. Patel and V. L. S. Chiang, "Laser interstitial thermal therapy for treatment of post-radiosurgery tumor recurrence and radiation necrosis," *Photonics Lasers Med.* **3**(2), 95 (2014).
34. S. Missios et al., "Prognostic factors of overall survival after laser interstitial thermal therapy in patients with glioblastoma," *Photonics Lasers Med.* **3**(2), 143 (2014).
35. W. Stummer, M. J. van den Bent, and M. Westphal, "Cytoreductive surgery of glioblastoma as the key to successful adjuvant therapies: new arguments in an old discussion," *Acta Neurochir. (Wien)* **153**(6), 1211-1218 (2011).
36. W. Stummer et al., "In vitro and in vivo porphyrin accumulation by C6 glioma cells after exposure to 5-aminolevulinic acid," *J. Photochem. Photobiol. B* **45**(2-3), 160-169 (1998).
37. W. Stummer et al., "Fluorescence-guided surgery with 5-aminolevulinic acid for resection of malignant glioma: a randomised controlled multicentre phase III trial," *Lancet Oncol.* **7**(5), 392-401 (2006).
38. M. Kriegmair et al., "Fluorescence cystoscopy following intravesical instillation of 5-aminolevulinic acid: a new procedure with high sensitivity for detection of hardly visible urothelial neoplasias," *Urol. Int.* **55**(4), 190-196 (1995).
39. M. Kriegmair et al., "Transurethral resection and surveillance of bladder cancer supported by 5-aminolevulinic acid-induced fluorescence endoscopy," *Eur. Urol.* **36**(5), 386-392 (1999).
40. W. Stummer et al., "Intraoperative detection of malignant gliomas by 5-aminolevulinic acid-induced porphyrin fluorescence," *Neurosurgery* **42**(3), 518-525; discussion 525-516 (1998).
41. W. Stummer et al., "Technical principles for protoporphyrin-IX-fluorescence guided microsurgical resection of malignant glioma tissue," *Acta Neurochir. (Wien)* **140**(10), 995-1000 (1998).
42. M. Loshchenov et al., "Endoscopic fluorescence visualization of 5-ALA photosensitized central nervous system tumors in the neural tissue transparency spectral range," *Photonics Lasers Med.* **3**(2), 159 (2014).
43. W. Stummer et al., "Fluorescence-guided resection of glioblastoma multiforme by using 5-aminolevulinic acid-induced porphyrins: a prospective study in 52 consecutive patients," *J. Neurosurg.* **93**(6), 1003-1013 (2000).
44. J. T. Liu, D. Meza, and N. Sanai, "Trends in fluorescence image-guided surgery for gliomas," *Neurosurgery* **75**(1), 61-71 (2014).
45. S. Eljamel et al., "Comparison of intraoperative fluorescence and MRI image guided neuronavigation in malignant brain tumours, a prospective controlled study," *Photodiagnosis Photodyn. Ther.* **10**(4), 356-361 (2013).
46. S. Zhao et al., "Intraoperative fluorescence-guided resection of high-grade malignant gliomas using 5-aminolevulinic acid-induced porphyrins: a systematic review and meta-analysis of prospective studies," *PLoS One* **8**(5), e63682 (2013).
47. G. Aldave et al., "Prognostic value of residual fluorescent tissue in glioblastoma patients after gross total resection in 5-aminolevulinic acid-guided surgery," *Neurosurgery* **72**(6), 915-920; discussion 920-911 (2013).
48. W. Stummer et al., "5-aminolevulinic acid-derived tumor fluorescence: the diagnostic accuracy of visible fluorescence qualities as corroborated by spectrometry and histology and postoperative imaging," *Neurosurgery* **74**(3), 310-319; discussion 319-320 (2014).
49. K. Svanberg et al., "Clinical and technical aspects of photodynamic therapy: superficial and interstitial illumination in skin and prostate cancer," in *Handbook of Biophotonics*, J. Popp et al., Eds., pp. 261-287, Wiley-VCH, Weinheim, Germany (2012).
50. B. Olzowy et al., "Photoirradiation therapy of experimental malignant glioma with 5-aminolevulinic acid," *J. Neurosurg.* **97**(4), 970-976 (2002).
51. S. Ito et al., "Oedema formation in experimental photo-irradiation therapy of brain tumours using 5-ALA," *Acta Neurochir. (Wien)* **147**(1), 57-65; discussion 65 (2005).
52. P. Zelenkov et al., "Acute morphological sequelae of photodynamic therapy with 5-aminolevulinic acid in the C6 spheroid model," *J. Neurooncol.* **82**(1), 49-60 (2007).
53. H. G. Stepp et al., "Fluorescence-guided resections and photodynamic therapy for malignant gliomas using 5-aminolevulinic acid," *Proc. SPIE* **5686**, 547-557 (2005).
54. Y. Lee and E. D. Baron, "Photodynamic therapy: current evidence and applications in dermatology," *Semin. Cutan. Med. Surg.* **30**(4), 199-209 (2011).
55. M. S. Eljamel, C. Goodman, and H. Moseley, "ALA and photofrin fluorescence-guided resection and repetitive PDT in glioblastoma multiforme: a single centre phase III randomised controlled trial," *Lasers Med. Sci.* **23**(4), 361-367 (2008).
56. L. Lilje and B. C. Wilson, "Photodynamic therapy of intracranial tissues: a preclinical comparative study of four different photosensitizers," *J. Clin. Laser Med. Surg.* **16**(2), 81-91 (1998).
57. L. Cui et al., "Porphyrin-lipid assembled HDL-like nanovesicles for fluorescence imaging and PDT treatment of orthotopic brain glioma tumor," presented at *Biomedical Optics 2014*, 26-30 April 2014, Miami, Florida, BT3A.55, Optical Society of America (2014).
58. S. L. Bisland et al., "Metronomic photodynamic therapy (mPDT) for intracranial neoplasm: physiological, biological, and dosimetry considerations," *Proc. SPIE* **5142**, 9-17 (2003).
59. S. K. Bisland et al., "Metronomic photodynamic therapy as a new paradigm for photodynamic therapy: rationale and preclinical evaluation of technical feasibility for treating malignant brain tumors," *Photochem. Photobiol.* **80**(1), 22-30 (2004).
60. T. J. Beck et al., "Interstitial photodynamic therapy of nonresectable malignant glioma recurrences using 5-aminolevulinic acid induced protoporphyrin IX," *Lasers Surg. Med.* **39**(5), 386-393 (2007).
61. A. Johansson et al., "Interstitial photodynamic therapy of brain tumors," *IEEE J. Sel. Topics Quantum Electron.* **16**(4), 841-853 (2010).
62. H. Stepp et al., "ALA and malignant glioma: fluorescence-guided resection and photodynamic treatment," *J. Environ. Pathol. Toxicol. Oncol.* **26**(2), 157-164 (2007).
63. W. Stummer et al., "Long-sustaining response in a patient with non-resectable, distant recurrence of glioblastoma multiforme treated by interstitial photodynamic therapy using 5-ALA: case report," *J. Neurooncol.* **87**(1), 103-109 (2008).
64. A. Johansson et al., "Protoporphyrin IX fluorescence and photobleaching during interstitial photodynamic therapy of malignant gliomas for early treatment prognosis," *Lasers Surg. Med.* **45**(4), 225-234 (2013).
65. B. Lai et al., "Characterization of a miniature integrating cylinder for absolute calibration of fluence rate probes for interstitial photodynamic therapy (IPDT)," *Proc. SPIE* **7373**, 73731M (2009).
66. A. Johansson et al., "ALA-mediated fluorescence-guided resection (FGR) and PDT of glioma," *Proc. SPIE* **7380**, 73801D (2009).
67. W. Göbel et al., "Optical needle endoscope for safe and precise stereotactically guided biopsy sampling in neurosurgery," *Opt. Express* **20**(24), 26117-26126 (2012).
68. A. Johansson et al., "Protoporphyrin IX for photodynamic therapy of brain tumours," *Proc. SPIE* **7715**, 77151M (2010).
69. G. Hennig, H. Stepp, and A. Johansson, "Photobleaching-based method to individualize irradiation time during interstitial 5-aminolevulinic acid photodynamic therapy," *Photodiagnosis Photodyn. Ther.* **8**(3), 275-281 (2011).
70. A. Rühm et al., "5-ALA based photodynamic management of glioblastoma," *Proc. SPIE* **8928**, 89280E (2014).
71. R. Siegel et al., "Cancer statistics, 2014," *CA Cancer J. Clin.* **64**(1), 9-29 (2014).
72. A. Jemal et al., "Global cancer statistics," *CA Cancer J. Clin.* **61**(2), 69-90 (2011).
73. "GLOBOCAN 2012: estimated cancer incidence, mortality and prevalence worldwide in 2012," 2014, http://globocan.iarc.fr/Pages/fact_sheets_cancer.aspx.
74. J. D. Campbell and S. D. Ramsey, "The costs of treating breast cancer in the USA synthesis of published evidence," *Pharmacoeconomics* **27**(3), 199-209 (2009).

75. Z. Kim et al., "The basic facts of Korean breast cancer in 2011: results of a nationwide survey and breast cancer registry database," *J. Breast Cancer* **17**(2), 99–106 (2014).
76. "Breast cancer screening programs in 26 ICSN countries, 2012: organization, policies, and program reach," 2012, <http://appliedresearch.cancer.gov/icsn/breast/screening.html>.
77. A. N. Freedman et al., "Cancer risk prediction models: a workshop on development, evaluation, and application," *JNCI* **97**(10), 715–723 (2005).
78. B. Rosner and G. A. Colditz, "Nurses' health study: log-incidence mathematical model of breast cancer incidence," *J. Natl. Cancer Inst.* **88**(6), 359–364 (1996).
79. N. F. Boyd et al., "Mammographic density and breast cancer risk: current understanding and future prospects," *Breast Cancer Res.* **13**(6) (2011).
80. Z. Aitken et al., "Screen-film mammographic density and breast cancer risk: a comparison of the volumetric standard mammogram form and the interactive threshold measurement methods," *Cancer Epidemiol. Biomarkers Prev.* **19**(2), 418–428 (2010).
81. E. J. Walter and L. Lilge, "Development of a modified transillumination breast spectroscopy (TiBS) system for population-wide screening," *Proc. SPIE* **7368**, 736820 (2009).
82. A. H. Gharekhan et al., "Characterizing fluorescence spectral features of cancer, benign and normal human breast tissues through wavelet transform and singular value decomposition," *Proc. SPIE* **7373**, 737300 (2009).
83. A. Poellinger, "Near-infrared imaging of breast cancer using optical contrast agents," *J. Biophotonics* **5**(11–12), 815–826 (2012).
84. L. Scolaro et al., "A review of optical coherence tomography in breast cancer," *Photonics Lasers Med.* **3**(3), 225 (2014).
85. P. Taroni et al., "Breast density assessment by means of time domain optical mammography at 635–1060 nm," *Proc. SPIE* **8088**, 80881E (2011).
86. P. Taroni et al., "Optical identification of subjects at high risk for developing breast cancer," *Proc. SPIE* **8799**, 87990O (2013).
87. K. M. Blackmore et al., "Estimation of mammographic density on an interval scale by transillumination breast spectroscopy," *J. Biomed. Opt.* **13**(6), 8 (2008).
88. K. Blyschak et al., "Classification of breast tissue density by optical transillumination spectroscopy: optical and physiological effects governing predictive value," *Med. Phys.* **31**(6), 1398–1414 (2004).
89. J. A. Knight et al., "Optical spectroscopy of the breast in premenopausal women reveals tissue variation with changes in age and parity," *Med. Phys.* **37**(2), 419–426 (2010).
90. N. F. Boyd et al., "Evidence that breast tissue stiffness is associated with risk of breast cancer," *Plos One* **9**(7), (2014).
91. A. Pettersson et al., "Mammographic density phenotypes and risk of breast cancer: a meta-analysis," *J. Natl. Cancer Inst.* **106**(5) (2014).
92. O. M. Ginsburg, L. J. Martin, and N. F. Boyd, "Mammographic density, lobular involution, and risk of breast cancer," *Br. J. Cancer* **99**(9), 1369–1374 (2008).
93. K. M. Blackmore, J. A. Knight, and L. Lilge, "Association between transillumination breast spectroscopy and quantitative mammographic features of the breast," *Cancer Epidemiol. Biomarkers Prev.* **17**(5), 1043–1050 (2008).
94. M. K. Simick and L. Lilge, "Optical transillumination spectroscopy to quantify parenchymal tissue density: an indicator for breast cancer risk," *Br. J. Radiol.* **78**(935), 1009–1017 (2005).
95. T. J. Farrell, M. S. Patterson, and B. Wilson, "A diffusion theory model of spatially resolved, steady-state diffuse reflectance for the noninvasive determination of tissue optical properties in vivo," *Med. Phys.* **19**(4), 879–888 (1992).
96. K. Blyschak et al., "Classification of breast tissue density by optical transillumination spectroscopy: optical and physiological effects governing predictive value," in *Applications of Photonic Technology 6: Closing the Gap between Theory, Development, and Application*, R. A. Lessard and G. A. Lampropoulos, Eds., pp. 568–579, SPIE Press, Bellingham, WA (2003).
97. L. Lilge et al., "Optical transillumination spectroscopy as biomarker for breast tissue density and cancer risk," *Cancer Epidemiol. Biomarkers Prev.* **13**(11), 1910S (2004).
98. M. K. Simick, B. C. Wilson, and L. D. Lilge, "Optical transillumination spectroscopy of breast tissue for cancer risk assessment," *Proc. SPIE* **4609**, 390–397 (2002).
99. J. E. Gunther et al., "Predicting tumor response in breast cancer patients using diffuse optical tomography," *Proc. SPIE* **8799**, 87990P (2013).
100. M. Alrubaiee et al., "Multi-wavelength diffusive optical tomography using independent component analysis and time reversal algorithms," *Proc. SPIE* **8088**, 80880Y (2011).
101. I. Bargigia et al., "Time-resolved diffuse optical spectroscopy up to 1700 nm using a time-gated InGaAs/InP single-photon avalanche diode," *Proc. SPIE* **8090**, 80900U (2011).
102. A. Pifferi et al., "Time-domain diffuse optical spectroscopy beyond 1100 nm: initial feasibility study," *Proc. SPIE* **8088**, 808817 (2011).
103. F. Tellier et al., "Comparison of 2- and 4-wavelength methods for the optical detection of sentinel lymph node," *Proc. SPIE* **8092**, 80920L (2011).
104. B. J. Tromberg et al., "Assessing the future of diffuse optical imaging technologies for breast cancer management," *Med. Phys.* **35**(6), 2443–2451 (2008).
105. J. Wang et al., "Near-infrared tomography of breast cancer hemoglobin, water, lipid, and scattering using combined frequency domain and cw measurement," *Opt. Lett.* **35**(1), 82–84 (2010).
106. C. Zhou et al., "Diffuse optical monitoring of blood flow and oxygenation in human breast cancer during early stages of neoadjuvant chemotherapy," *J. Biomed. Opt.* **12**(5), 051903 (2007).
107. Y. Lin, O. Nalcioglu, and G. Gulsen, "Fiber bundle based fluorescence tomography system for human breast imaging," *Proc. SPIE* **7371**, 737108 (2009).
108. V. Piron and J.-P. L'Huillier, "Resolution limits between objects embedded in breast-like slab using the optical frequency-domain method: a numerical approach," *Proc. SPIE* **8092**, 80920O (2011).
109. M. Guven et al., "Diffuse optical tomography with a priori anatomical information," *Phys. Med. Biol.* **50**(12), 2837–2858 (2005).
110. A. Li et al., "Optimal linear inverse solution with multiple priors in diffuse optical tomography," *Appl. Opt.* **44**(10), 1948–1956 (2005).
111. P. K. Yalavarthy et al., "Structural information within regularization matrices improves near infrared diffuse optical tomography," *Opt. Express* **15**(13), 8043–8058 (2007).
112. H. Soliman et al., "Functional imaging using diffuse optical spectroscopy of neoadjuvant chemotherapy response in women with locally advanced breast cancer," *Clin. Cancer Res.* **16**(9), 2605–2614 (2010).
113. M. Heijblom et al., "Breast imaging using the Twente Photoacoustic Mammoscope (PAM): new clinical measurements," *Proc. SPIE* **8087**, 80870N (2011).
114. M. Heijblom et al., "Photoacoustic imaging of breast tumor vascularization: a comparison with MRI and histopathology," *Proc. SPIE* **8800**, 880004 (2013).
115. T. Kitai et al., "Photoacoustic mammography: initial clinical results," *Breast Cancer* **21**(2), 146–153 (2014).
116. R. G. Pleijhuis et al., "Obtaining adequate surgical margins in breast-conserving therapy for patients with early-stage breast cancer: current modalities and future directions," *Ann. Surg. Oncol.* **16**(10), 2717–2730 (2009).
117. J. S. D. Mieog et al., "Image-guided tumor resection using real-time near-infrared fluorescence in a syngeneic rat model of primary breast cancer," *Breast Cancer Res. Treat.* **128**(3), 679–689 (2011).
118. J. S. D. Mieog et al., "Novel intraoperative near-infrared fluorescence camera system for optical image-guided cancer surgery," *Mol. Imaging* **9**(4), 223–231 (2010).
119. B. E. Schaafsma et al., "The clinical use of indocyanine green as a near-infrared fluorescent contrast agent for image-guided oncologic surgery," *J. Surg. Oncol.* **104**(3), 323–332 (2011).
120. W. B. Guo et al., "Breast cancer sentinel lymph node mapping using near-infrared guided indocyanine green in comparison with blue dye," *Tumor Biol.* **35**(4), 3073–3078 (2014).
121. N. Haj-Hosseini et al., "Fluorescence spectroscopy using indocyanine green for lymph node mapping," *Proc. SPIE* **8935**, 893504 (2014).
122. F. P. R. Verbeek et al., "Near-infrared fluorescence sentinel lymph node mapping in breast cancer: a multicenter experience," *Breast Cancer Res. Treat.* **143**(2), 333–342 (2014).

123. L. Xiong et al., "Indocyanine green fluorescence-guided sentinel node biopsy: a meta-analysis on detection rate and diagnostic performance," *EJSO* **40**(7), 843–849 (2014).
124. Z. Huang, "A review of progress in clinical photodynamic therapy," *Technol. Cancer Res. Treat.* **4**(3), 283–293 (2005).
125. J. D. Miller et al., "Photodynamic therapy with the phthalocyanine photosensitizer Pc 4: the case experience with preclinical mechanistic and early clinical-translational studies," *Toxicol. Appl. Pharmacol.* **224**(3), 290–299 (2007).
126. K. H. Haraldsdottir et al., "Interstitial laser thermotherapy (ILT) of breast cancer," *EJSO* **34**(7), 739–745 (2008).
127. S. C. Jiang and X. X. Zhang, "Dynamic modeling of photothermal interactions for laser-induced interstitial thermotherapy: parameter sensitivity analysis," *Lasers Med. Sci.* **20**(3–4), 122–131 (2005).
128. H. Choi and Z. Tovar-Spinoza, "MRI-guided laser interstitial thermal therapy of intracranial tumors and epilepsy: state-of-the-art review and a case study from pediatrics," *Photonics Lasers Med.* **3**(2), 107 (2014).
129. D. S. Robinson et al., "Interstitial laser hyperthermia model development for minimally invasive therapy of breast carcinoma," *J. Am. Coll. Surg.* **186**(3), 284–292 (1998).
130. T. Schroder et al., "Percutaneous interstitial laser hyperthermia in clinical use," *Ann. Chir. Gynaecol.* **83**(4), 286–290 (1994).
131. K. G. Tranberg, "Laser tumor thermotherapy: is there a clinically relevant effect on the immune system?," *Proc. SPIE* **6087**, 60870B (2006).
132. M. K. Akens et al., "Photodynamic therapy of vertebral metastases: evaluating tumor-to-neural tissue uptake of BPD-MA and ALA-PpIX in a murine model of metastatic human breast carcinoma," *Photochem. Photobiol.* **83**(5), 1034–1039 (2007).
133. N. Batista and D. Liang, "A simple color separation technique for solar tissue photocoagulation," *Proc. SPIE* **8092**, 80921K (2011).
134. C. W. Chang and W. R. Ries, "Surgical treatment of the inferior turbinate: new techniques," *Curr. Opin. Otolaryngol. Head Neck Surg.* **12**(1), 53–57 (2004).
135. R. Mladina, R. Risavi, and M. Subaric, "CO₂ laser anterior turbinectomy in the treatment of non-allergic vasomotor rhinopathy. A prospective study upon 78 patients," *Rhinology* **29**(4), 267–271 (1991).
136. A. DeRowe et al., "Subjective comparison of Nd:YAG, diode, and CO₂ lasers for endoscopically guided inferior turbinate reduction surgery," *Am. J. Rhinol.* **12**(3), 209–212 (1998).
137. E. Serrano et al., "The holmium:YAG laser for treatment of inferior turbinate hypertrophy," *Rhinology* **36**(2), 77–80 (1998).
138. A. Leunig et al., "Ho:YAG laser treatment of hyperplastic inferior nasal turbinates," *Laryngoscope* **109**(10), 1690–1695 (1999).
139. P. Janda et al., "Laser treatment of hyperplastic inferior nasal turbinates: a review," *Lasers Surg. Med.* **28**(5), 404–413 (2001).
140. R. Sroka et al., "Endonasal laser surgery with a new laser fiber guidance instrument," *Laryngoscope* **110**(2 Pt 1), 332–334 (2000).
141. M. Havel et al., "A double-blind, randomized, intra-individual controlled feasibility trial comparing the use of 1, 470 and 940 nm diode laser for the treatment of hyperplastic inferior nasal turbinates," *Lasers Surg. Med.* **43**(9), 881–886 (2011).
142. R. Sroka et al., "Controlled feasibility trial comparing the use of 1470 nm and 940 nm diode laser for the treatment of hyperplastic inferior nasal turbinates," *Proc. SPIE* **8207**, 82072Y (2012).
143. C. S. Betz et al., "Coagulative and ablative characteristics of a novel diode laser system (1470 nm) for endonasal applications," *Proc. SPIE* **6842**, 68421Z (2008).
144. R. Sroka et al., "Clinical feasibility trial on 1940 nm Tm: fiber laser intervention of hyperplastic inferior nasal turbinates," *Photonics Lasers Med.* **1**(3), 215 (2012).
145. P. Janda et al., "Comparison of thermal tissue effects induced by contact application of fiber guided laser systems," *Lasers Surg. Med.* **33**(2), 93–101 (2003).
146. P. Janda et al., "Diode laser treatment of hyperplastic inferior nasal turbinates," *Lasers Surg. Med.* **27**(2), 129–139 (2000).
147. J. Newman and V. Anand, "Applications of the diode laser in otolaryngology," *Ear Nose Throat J.* **81**(12), 850–851 (2002).
148. D. Passali et al., "Treatment of inferior turbinate hypertrophy: a randomized clinical trial," *Ann. Otol. Rhinol. Laryngol.* **112**(8), 683–688 (2003).
149. S. D. Rejali et al., "Inferior turbinate reduction in children using holmium YAG laser—a clinical and histological study," *Lasers Surg. Med.* **34**(4), 310–314 (2004).
150. R. Sroka et al., "Comparison of long term results after Ho:YAG and diode laser treatment of hyperplastic inferior nasal turbinates," *Lasers Surg. Med.* **39**(4), 324–331 (2007).
151. R. Sroka et al., "Laser treatment of hyperplastic inferior nasal turbinates: 1 year follow up," presented at *Biomedical Topical Meeting*, 14 June 1999, Munich, Germany, CWD5, Optical Society of America.
152. P. Janda et al., "Comparison of laser induced effects on hyperplastic inferior nasal turbinates by means of scanning electron microscopy," *Lasers Surg. Med.* **30**(1), 31–39 (2002).
153. R. Sroka et al., "Treatment of hyperplastic inferior nasal turbinates by means of a Ho:YAG laser," *Proc. SPIE* **3590**, 229–232 (1999).
154. C. J. Nease and G. A. Kreml, "Radiofrequency treatment of turbinate hypertrophy: a randomized, blinded, placebo-controlled clinical trial," *Otolaryngol. Head Neck Surg.* **130**(3), 291–299 (2004).
155. M. Cavaliere, G. Mottola, and M. Iemma, "Monopolar and bipolar radiofrequency thermal ablation of inferior turbinates: 20-month follow-up," *Otolaryngol. Head Neck Surg.* **137**(2), 256–263 (2007).
156. N. D. Bhandarkar and T. L. Smith, "Outcomes of surgery for inferior turbinate hypertrophy," *Curr. Opin. Otolaryngol. Head Neck Surg.* **18**(1), 49–53 (2010).
157. D. Willatt, "The evidence for reducing inferior turbinates," *Rhinology* **47**(3), 227–236 (2009).
158. P. P. Caffier et al., "Rhinitis medicamentosa: therapeutic effect of diode laser inferior turbinate reduction on nasal obstruction and decongestant abuse," *Am. J. Rhinol.* **22**(4), 433–439 (2008).
159. G. F. Volk et al., "Prognostic value of anterior rhinomanometry in diode laser turbinoplasty," *Arch. Otolaryngol. Head Neck Surg.* **136**(10), 1015–1019 (2010).
160. L. Navarro, R. J. Min, and C. Bone, "Endovenous laser: a new minimally invasive method of treatment for varicose veins: preliminary observations using an 810 nm diode laser," *Dermatol. Surg.* **27**(2), 117–122 (2001).
161. R. J. Min et al., "Endovenous laser treatment of the incompetent greater saphenous vein," *J. Vasc. Interv. Radiol.* **12**(10), 1167–1171 (2001).
162. W. S. Malskat et al., "Endovenous laser ablation (EVLA): a review of mechanisms, modeling outcomes, and issues for debate," *Lasers Med. Sci.* **29**(2), 393–403 (2014).
163. W. S. Malskat et al., "Temperature profiles of 980- and 1, 470-nm endovenous laser ablation, endovenous radiofrequency ablation and endovenous steam ablation," *Lasers Med. Sci.* **29**(2), 423–429 (2014).
164. A. B. Massaki et al., "Endoluminal laser delivery mode and wavelength effects on varicose veins in an ex vivo model," *Lasers Surg. Med.* **45**(2), 123–129 (2013).
165. M. Heger et al., "Endovascular laser-tissue interactions and biological responses in relation to endovenous laser therapy," *Lasers Med. Sci.* **29**(2), 405–422 (2014).
166. R. Sroka et al., "Ex-vivo investigations on endoluminal vein treatment procedures," *Proc. SPIE* **6424**, 64240M (2007).
167. R. Sroka et al., "The ox-foot-model for investigating endoluminal thermal treatment modalities of varicosis vein diseases," *ALTEX* **29**(4), 403–410 (2012).
168. R. Sroka et al., "Endovenous laser therapy—application studies and latest investigations," *J. Biophotonics* **3**(5–6), 269–276 (2010).
169. R. Brar et al., "Surgical management of varicose veins: meta-analysis," *Vascular* **18**(4), 205–220 (2010).
170. C. Carroll et al., "Systematic review, network meta-analysis and exploratory cost-effectiveness model of randomized trials of minimally invasive techniques versus surgery for varicose veins," *Br. J. Surg.* **101**(9), 1040–1052 (2014).
171. N. P. Lynch, M. Clarke, and G. J. Fulton, "Surgical management of great saphenous vein varicose veins: a meta-analysis," *Vascular* (2014).
172. C. Nesbitt et al., "Endovenous ablation (radiofrequency and laser) and foam sclerotherapy versus open surgery for great saphenous vein varices," *Cochrane Database Syst. Rev.* **7**, CD005624 (2014).
173. Y. Pan et al., "Comparison of endovenous laser ablation and high ligation and stripping for varicose vein treatment: a meta-analysis," *Phlebology* **29**(2), 109–119 (2014).

174. B. Siribumrungwong et al., "A systematic review and meta-analysis of randomised controlled trials comparing endovenous ablation and surgical intervention in patients with varicose vein," *Eur. J. Vasc. Endovasc. Surg.* **44**(2), 214–223 (2012).
175. R. van den Bos et al., "Endovenous therapies of lower extremity varicosities: a meta-analysis," *J. Vasc. Surg.* **49**(1), 230–239 (2009).
176. R. Sroka et al., "Endovenous laser application. Strategies to improve endoluminal energy application," *Phlebologie* **42**(3), 121–129 (2013).
177. C. M. Fan and R. Rox-Anderson, "Endovenous laser ablation: mechanism of action," *Phlebologie* **23**(5), 206–213 (2008).
178. M. E. Vuylsteke and S. R. Mordon, "Endovenous laser ablation: a review of mechanisms of action," *Ann. Vasc. Surg.* **26**(3), 424–433 (2012).
179. M. J. van Gemert et al., "Comment to Vuylsteke ME and Mordon SR. Endovenous laser ablation: a review of mechanisms of action. *Ann Vasc Surg* 2012;26:424-33," *Ann. Vasc. Surg.* **26**(6), 881–883 (2012).
180. T. M. Proebstle, T. Moehler, and S. Herdemann, "Reduced recanalization rates of the great saphenous vein after endovenous laser treatment with increased energy dosing: definition of a threshold for the endovenous fluence equivalent," *J. Vasc. Surg.* **44**(4), 834–839 (2006).
181. T. Stokbroekx et al., "Commonly used fiber tips in endovenous laser ablation (EVLA): an analysis of technical differences," *Lasers Med. Sci.* **29**(2), 501–507 (2014).
182. S. R. Mordon, B. Wassmer, and J. Zemmouri, "Mathematical modeling of 980-nm and 1320-nm endovenous laser treatment," *Lasers Surg. Med.* **39**(3), 256–265 (2007).
183. S. R. Mordon, B. Wassmer, and J. Zemmouri, "Mathematical modeling of endovenous laser treatment (ELT)," *Biomed. Eng. Online* **5**, 26 (2006).
184. P. W. van Ruijven et al., "Optical-thermal mathematical model for endovenous laser ablation of varicose veins," *Lasers Med. Sci.* **29**(2), 431–439 (2014).
185. A. A. Poluektova et al., "Some controversies in endovenous laser ablation of varicose veins addressed by optical-thermal mathematical modeling," *Lasers Med. Sci.* **29**(2), 441–452 (2014).
186. V. P. Minaev et al., "Endovenous laser treatment (EVLT) of saphenous vein reflux with 1.56 μm laser," *Proc. SPIE* **7373**, 73731D (2009).
187. C. G. Schmedt et al., "Evaluation of endovenous radiofrequency ablation and laser therapy with endoluminal optical coherence tomography in an ex vivo model," *J. Vasc. Surg.* **45**(5), 1047–1058 (2007).
188. C. G. Schmedt et al., "Investigation on radiofrequency and laser (980 nm) effects after endoluminal treatment of saphenous vein insufficiency in an ex-vivo model," *Eur. J. Vasc. Endovasc. Surg.* **32**(3), 318–325 (2006).
189. N. Bosschaart et al., "A literature review and novel theoretical approach on the optical properties of whole blood," *Lasers Med. Sci.* **29**(2), 453–479 (2014).
190. R. Sroka et al., "Ex-vivo investigation of endoluminal vein treatment by means of radiofrequency and laser irradiation," *Med. Laser Appl.* **21**(1), 15–22 (2006).
191. N. Topaloglu et al., "Comparison of 980-nm and 1070-nm in endovenous laser treatment (EVLT)," *Proc. SPIE* **7373**, 73731S (2009).
192. R. Baumgartner et al., "Tissue laser ablation process and device," Germany, WO1998032381 A1 (1998).
193. F. Pannier, E. Rabe, and U. Maurins, "First results with a new 1470-nm diode laser for endovenous ablation of incompetent saphenous veins," *Phlebologie* **24**(1), 26–30 (2009).
194. U. Maurins, E. Rabe, and F. Pannier, "Does laser power influence the results of endovenous laser ablation (EVLA) of incompetent saphenous veins with the 1470-nm diode laser? A prospective randomized study comparing 15 and 25 W," *Int. Angiol.* **28**(1), 32–37 (2009).
195. S. Doganci and U. Demirkilic, "Comparison of 980 nm laser and bare-tip fibre with 1470 nm laser and radial fibre in the treatment of great saphenous vein varicosities: a prospective randomised clinical trial," *Eur. J. Vasc. Endovasc. Surg.* **40**(2), 254–259 (2010).
196. F. Pannier et al., "Endovenous laser ablation of great saphenous veins using a 1470 nm diode laser and the radial fibre: follow-up after six months," *Phlebologie* **26**(1), 35–39 (2011).
197. T. Schwarz et al., "Endovenous laser ablation of varicose veins with the 1470-nm diode laser," *J. Vasc. Surg.* **51**(6), 1474–1478 (2010).
198. M. Vuylsteke et al., "Endovenous laser treatment: is there a clinical difference between using a 1500 nm and a 980 nm diode laser? A multicenter randomised clinical trial," *Int. Angiol.* **30**(4), 327–334 (2011).
199. M. Mozafar et al., "Endovenous laser ablation of the great saphenous vein versus high ligation: long-term results," *Lasers Med. Sci.* **29**(2), 765–771 (2014).
200. R. R. van den Bos and T. M. Proebstle, "The state of the art of endothermal ablation," *Lasers Med. Sci.* **29**(2), 387–392 (2014).
201. E. von Hodenberg et al., "Endovenous laser ablation of varicose veins with the 1470 nm diode laser using a radial fiber: 1-year follow-up," *Phlebologie* **30**(2), 86–90 (2015).
202. P. Gloviczki et al., "The care of patients with varicose veins and associated chronic venous diseases: clinical practice guidelines of the Society for Vascular Surgery and the American Venous Forum," *J. Vasc. Surg.* **53**(5 Suppl), 2S–48S (2011).
203. National Clinical Guideline Centre, *Varicose Veins in the Legs. The Diagnosis and Management of Varicose Veins*, National Institute for Health and Care Excellence, London, United Kingdom (2013).
204. K. Rass et al., "Comparable effectiveness of endovenous laser ablation and high ligation with stripping of the great saphenous vein: two-year results of a randomized clinical trial (RELACS study)," *Arch. Dermatol.* **148**(1), 49–58 (2012).
205. J. P. Tesmann et al., "Radiofrequency induced thermotherapy (RFITT) of varicose veins compared to endovenous laser treatment (EVLT): a non-randomized prospective study concentrating on occlusion rates, side-effects and clinical outcome," *Eur. J. Dermatol.* **21**(6), 945–951 (2011).
206. L. H. Rasmussen et al., "Randomized clinical trial comparing endovenous laser ablation, radiofrequency ablation, foam sclerotherapy and surgical stripping for great saphenous varicose veins," *Br. J. Surg.* **98**(8), 1079–1087 (2011).
207. B. C. Disselhoff et al., "Five-year results of a randomized clinical trial comparing endovenous laser ablation with cryostripping for great saphenous varicose veins," *Br. J. Surg.* **98**(8), 1107–1111 (2011).
208. B. C. Disselhoff et al., "Five-year results of a randomised clinical trial of endovenous laser ablation of the great saphenous vein with and without ligation of the saphenofemoral junction," *Eur. J. Vasc. Endovasc. Surg.* **41**(5), 685–690 (2011).
209. T. Luebke and J. Brunkwall, "Systematic review and meta-analysis of endovenous radiofrequency obliteration, endovenous laser therapy, and foam sclerotherapy for primary varicosis," *J. Cardiovasc. Surg. (Torino)* **49**(2), 213–233 (2008).
210. T. Luebke et al., "Meta-analysis of endovenous radiofrequency obliteration of the great saphenous vein in primary varicosis," *J. Endovasc. Ther.* **15**(2), 213–223 (2008).
211. R. Sroka et al., "Endovenous laser application. possibilities of online monitoring," *Phlebologie* **42**(3), 131–138 (2013).

Ronald Sroka received his physics diploma at the Georg-August-University of Göttingen, Germany, and his PhD degree in the field of photodynamic therapy at the University of Munich, Germany. His research is focused on various aspects of photodynamic therapy and on thermal laser applications in a variety of clinical disciplines. Since 2010, he has been the head of the Laser-Forschungslabor in the LIFE Center at the hospital of the University of Munich.

Herbert Stepp received his diploma in physics in 1984 and has worked since then on photodynamic procedures. He obtained his PhD degree at the medical faculty of the University of Munich and became a research group leader at the LIFE Center in 1993. His research focuses on optics-based methods for the detection of cancer and other disorders. His research on 5-aminolevulinic acid based fluorescence techniques contributed to the approvals of fluorescence cystoscopy and fluorescence-guided resection of malignant glioma.

Georg Hennig is a physicist at the Laser-Forschungslabor, Klinikum der Universität München. He received his PhD degree in the field of fluorescence diagnostics. He currently focuses on medical device development and evaluation.

Gary M. Brittenham is the James A. Wolff professor of pediatrics and professor of medicine at the Columbia University College of Physicians and Surgeons. His research interests involve basic and clinical research in disorders of the red blood cell and of iron metabolism. His laboratory has helped develop noninvasive means for the measurement of tissue iron using magnetic susceptometry and magnetic resonance methods.

Adrian Rühm received his diploma in physics in 1993 and his PhD degree in 1998, at the Universities of München and Wuppertal, Germany, respectively. He worked in materials science with x-rays and neutrons in Stuttgart and Garching, Germany, and in Chicago, United States. In 2011, he joined the Laser-Forschungslabor in München, Germany, to conduct research in the field of biophotonics for medical applications. His current research activities are focused on photodynamic therapy and *in vivo* photodiagnosis.

Lothar Lilge completed his initial training at the University of Frankfurt, Germany, in the group of Dr. Hillenkamp. He worked at the Wellman Laboratory of Photomedicine in Boston, United States, and as a postdoc at McMaster University in Hamilton, Canada. His main research thrust pertains to photodynamic therapy in oncology, diffuse reflectance for breast cancer risk assessment, and microfluidics for single-cell analysis. Currently, he is a senior scientist at the Princess Margaret Cancer Centre and professor at the University of Toronto.